

LEARNING ERDŐS-RÉNYI GRAPHS UNDER PARTIAL OBSERVATIONS: CONCENTRATION OR SPARSITY?

BY VINCENZO MATTA^{*}, AUGUSTO SANTOS[†] AND ALI H. SAYED[†]

DIEM^{} and EPFL[†]*

This work examines the problem of graph learning over a diffusion network when data can be collected from a limited portion of the network (*partial observability*). While most works in the literature rely on a degree of sparsity to provide guarantees of consistent graph recovery, our analysis moves away from this condition and includes the demanding setting of *dense* connectivity. We ascertain that suitable estimators of the combination matrix (i.e., the matrix that quantifies the pairwise interaction between nodes) possess an *identifiability gap* that enables the discrimination between connected and disconnected nodes. Fundamental conditions are established under which the subgraph of monitored nodes can be recovered, with high probability as the network size increases, through *universal* clustering algorithms. This claim is proved for three matrix estimators: *i*) the Granger estimator that adapts to the partial observability setting the solution that is optimal under full observability ; *ii*) the one-lag correlation matrix; and *iii*) the residual estimator based on the difference between two consecutive time samples. Comparison among the estimators is performed through illustrative examples that reveal how estimators that are not optimal in the full observability regime can outperform the Granger estimator in the partial observability regime. The analysis reveals that the fundamental property enabling consistent graph learning is the *statistical concentration* of node degrees, rather than the sparsity of connections.

1. Introduction. Learning the graph structure that governs the evolution of a networked dynamical system from data collected at some accessible nodes is a challenging inverse problem with applications across many domains. The objective of such inferential problems is to discover the interaction profile among the network nodes since the topology has a critical effect on system behavior [4]. Graph learning plays a central role in many applications including, among other possibilities: estimating the longevity or the source of an epidemics [34]; revealing commonalities and agent influence over social networks [19]; discovering the routes of clandestine information flows [41]; identifying defective elements [11]; addressing the fundamental

Keywords and phrases: Graph learning, network tomography, dense networks, Granger estimator, diffusion network, Erdős-Rényi graph, identifiability gap, graph concentration.

issue in neuroscience that links brain functional connectivity (i.e., a “functional” topology estimated from blood-oxygenation-level-dependent signals) to brain structural connectivity (i.e., the anatomical topology of neuron interconnections) [18].

Depending on the particular context, the aforementioned class of problems can be referred to in different ways, including *topology inference* [20], *network tomography* [28, 36], *structure learning*, or *graph learning* [2]. We adopt these terminologies almost interchangeably throughout our treatment.

This article addresses the graph learning problem under the framework of *partial observability*, i.e., when only a fraction of the network nodes can be probed. Providing technical guarantees of graph learning under such a demanding setting is critical in large-scale networked systems, where it is not feasible to gather data from all nodes comprising the network. Furthermore, we solve the learning problem for distinct regimes of network wiring, including *densely-connected* networks, a case often overlooked in the literature and challenging to be addressed in general.

We establish that, over a diffusion network, and under certain assumptions on the generative model — i.e., on the entries of the combination matrix and its underlying support graph — the problem of topology inference becomes *local*, i.e., all the information about the underlying subnetwork connecting the observed agents is contained in the samples of the observed agents, asymptotically as the network size gets large, and irrespective of the density of connections.

2. Overview of the Learning Problem. The structure of the learning problem addressed in this work can be summarized as follows. Streams of data originating from a certain subnetwork are collected, and the goal is to estimate the (unknown) topology linking the nodes of this subnetwork from the collected data. The graph learning protocol will involve two main steps: an estimation step, where a combination matrix (i.e., a matrix quantifying the strength of the connections among the network nodes) is estimated; and a thresholding step, where node pairs linked by a strong edge (i.e., node pairs whose corresponding combination matrix entry lies above some threshold) are deemed connected. A structurally-consistent estimator is one that ends up assigning strong ties to interacting pairs and weak ties to non-interacting pairs. In this way, at the thresholding stage, one can correctly classify the pairs as interacting and non-interacting.

It is useful to illustrate the learning problem in relation to some popular networked systems. To start with, let us neglect some practical limitations, in particular: *i*) assume that all nodes can be monitored (full observability);

ii) that there are no limitations in terms of computational power; and *iii*) there are no limitations on the available time samples. Then, the first inferential stage consists of finding a matrix estimator to quantify the strength of pairwise interactions in the network. One notable estimator relies on computing the (spatial) correlation matrix $R_0 = \lim_{n \rightarrow \infty} \mathbb{E} [\mathbf{y}_n \mathbf{y}_n^\top]$, where \mathbf{y}_n denotes the vector collecting the data from all nodes at time n , and where assumption *iii*) above justifies the limit and (under an ergodic assumption) implies that the statistical average can be learned from the data. When the matrix R_0 provides a consistent estimator for the connection strengths, we talk of a *correlation network* [20]. For these networks, interactions between two nodes are *direct* and they are directly captured from pairwise correlations. One example of a correlation network is the ferromagnetic Ising model [5] with independent and identically distributed (i.i.d.) time samples, and under certain constraints of sparsity on the network and of regularity on the weights of interaction.

Another classic model for graph learning is a *Gaussian graphical model*. In this case, R_0 is no longer the proper estimator, but its inverse R_0^{-1} (which is often referred to as the precision or concentration matrix) is a consistent estimator, in that its support coincides with the underlying graph of interactions. Over Gaussian graphical models, the pairwise interaction between adjacent nodes is affected by other nodes, and this latent influence is the reason why spatial correlation between measurements is no longer sufficient to capture the network structure.

For most standard graphical models, pairwise interactions are described through dependent random variables defined on the network nodes. It is usually assumed that i.i.d. samples of these variables are available for the learning process. In other words, over graphical models the data samples do not arise from a dynamical process governing the time evolution of the nodes' outputs. In contrast, there is the more interesting class of graph models that correspond to dynamical graph systems. In this case, the signal time-evolution at any node is influenced by the signal evolutions at neighboring nodes. One relevant example is the diffusion or first-order Vector Autoregressive (VAR) system described by (4.2) further ahead. For such graphs, the proper estimator for graph connectivity turns out to be the Granger estimator, $R_1 R_0^{-1}$, which combines in a suitable way information contained in the correlation matrix, R_0 , and in the *one-lag* correlation matrix, R_1 .

In this article, we will be dealing with dynamic graphs, where signals evolve at the nodes and are affected by the evolution of the signals at neighboring agents as well.

2.1. *Structural-Consistency, Hardness, and Sample-Complexity.* We are now ready to introduce three concepts that play an important role in graph learning problems.

Structural consistency. If it is possible to discover the graph structure from a statistical descriptor related to the measurements (in the previous examples, R_0 , R_0^{-1} , or $R_1R_0^{-1}$), we shall say that the graph learning problem is *identifiable*. When a graph learning problem is identifiable, the goal is to find a matrix estimator that is able to guess the correct graph. Given a matrix estimator that allows identifying (at least asymptotically as the network size goes to infinity) the graph structure, we shall say that this matrix estimator achieves *structural consistency*. We see that identifiability is a property of a given graph learning problem, whereas consistency is a property of a given matrix estimator applied to an identifiable problem.

In this work we focus on the case in which the measurements are available from only a limited subset of nodes, with identifiability referring here to the subgraph connecting these monitored nodes. The identifiability issue becomes particularly critical under this demanding setting, giving rise to many interesting as well as challenging questions, such as: *Does partial observability impair identifiability of the monitored subnetwork? If not, how can we design structurally-consistent estimators?*

We remark that the concepts of identifiability and structural consistency disregard complexity issues, since they assume that the necessary statistical quantities are available. For example, we assume that $R_1R_0^{-1}$ can be computed exactly, which means that we have sufficient time to learn and that matrix inversion is possible whatever the size of the network.

Hardness. How much complexity is required to evaluate the matrix estimator necessary for a particular graph learning problem? For example, if one is interested in the precision matrix, R_0^{-1} , the hardness is related to the complexity of the matrix inversion. Many works attempt to reduce the complexity by leveraging particular constraints such as smoothness or sparsity of the graph signals. Notably, the problem of topology inference under partial observability is in general not feasible or NP-hard [9, 12], particularly over *loopy* or non-tree like graphs. The present work sheds light on a class of networked systems whereby structure learning of the observable subgraph is not only feasible but is not “so hard” as it provides technical guarantees of consistency for estimators of affordable complexity, even over the hardly explored and nonetheless of critical importance *densely connected networks* — thus, loopy and non-tree like. We remark that the concept of hardness disregards the complexity associated with the *empirical* estimation

of the pertinent matrices from the available data samples. This element of complexity is usually referred to as *sample* complexity.

Sample complexity. In practice, only a finite amount of data is available and, therefore, only approximate versions of the aforementioned matrix estimators can be computed. There exist several results about sample complexity in the context of high-dimensional graphical models, where the number of samples necessary to get some prescribed accuracy is related to the system parameters, e.g., to the network size and to the density of connections. In contrast, results relative to sample complexity are less mature over dynamical graph systems, including the systems considered in this work [20]. In order to avoid confusion, we remark that we will not deal with an analytical characterization of sample complexity. We touch upon this aspect in the section devoted to numerical experiments, where we examine the performance of the proposed learning strategies over finite data streams.

3. Related Work.

3.1. *Learning under Full Observability.* The majority of works on graph learning over networks focuses on linear system dynamics, with nonlinear dynamics typically being tackled by variational characterizations under a small-noise assumption [32], or by increasing the dimensionality of the observable space [29].

Topology inference for a general class of linear stochastic dynamical systems (e.g., VAR models of arbitrary order, or even non-causal linear models) is addressed in [21]. An approach based on Wiener filtering is proposed to infer the topology, which provides exact reconstruction for self-kin networks or, in general, guarantees reconstruction of the smallest self-kin network embracing the true network.

There exist works dealing with more general dynamical systems and graphs. For example, in [35] the concept of directed information graphs is advocated to discover dependencies in networks of interacting processes linked by causal dynamics. And a metric to learn causal relationships by means of *functional dependencies* is proposed in [15] to track the graph structure over a possibly nonlinear network.

Moving closer to our setting, among linear (or linearized) systems, special attention is devoted to autoregressive diffusion models [17, 30, 31, 33, 40]. For instance, in [30] causal graph processes are exploited to devise a computationally tractable algorithm for graph structure recovery with performance guarantees. Recent works exploit optimization and graph signal processing techniques to feed the graph learning algorithm with proper structural con-

straints. In [33,40], it is shown how to capitalize on the fact that the weighting matrix and the correlation matrix share the same eigenvectors, and how to solve the topology inverse problem through optimization methods under sparsity constraints. An account of the methods for the full observability regime can be found in [20].

We stress that most of the aforementioned methods work in the *graph spectral domain*. This has to be contrasted with the methods proposed in this paper, which rely instead on the graph edge domain. Working in the edge domain allows us to obtain a transparent relationship for the matrix estimators, which is critical to establish identifiability under the challenging partial observability setting.

In summary, while in certain cases (e.g., general linear models and/or non-linear models) identifiability can be an issue, most of the works on diffusion models focus on reducing complexity by exploiting proper structural constraints (e.g., smoothness or sparsity of the signals defined on the graph) [20]. However, all the aforementioned results pertain to the case where node measurements from the entire network are available. We focus instead on the case in which only partial observation of the network is permitted.

3.2. Learning under Partial Observability. A fundamental challenge of our work is performing structure learning when only *partial* observation is allowed. Under this setting, results for retrieving particular network graphs (polytrees) are available in [22] and [16]. Considering instead the case of general topologies, and with focus on VAR/diffusion models like the one considered in this work, references [17,23] establish technical conditions for exact or partial topology identifiability. However, these identifiability conditions act at a very “microscopic” level (they are formulated in terms of some precise details of the local graph structure and/or of the statistical model), and are therefore impractical over large-scale networks. In contrast, in this work we pursue a statistical asymptotic approach that is genuinely tailored to the large-scale setting: an asymptotic (i.e., large-network) framework is considered, where a thermodynamic limit of large graphs is afforded by using *random* graphs, and the conditions on the network connection topology are summarized at a *macroscopic* level through average descriptive indicators (e.g., probability of drawing an edge). In a similar vein, detailed asymptotic analysis with performance guarantees are available for graphical models with latent variables. For example, in [10] it is shown that, under certain conditions concerning the interactions between the observed and the unobserved network nodes, the “*sparsity+low-rank*” framework can be exploited to estimate the amount of latent variables [10], and to reconstruct the topology

of the observable subnetwork. Likewise, in [2] the graph learning problem is tackled in the context of locally-tree graphs, whereas in [1] a local separation criterion is imposed to deal with Gaussian graphical models.

However, and as already explained in Sec.2, graphical models do not match the networked dynamical models considered in this work. For these models, results for graph learning under partial observation have been recently obtained in [26, 28, 36–38]. More specifically, *i*) in [28] the whole network graph is assumed to follow an Erdős-Rényi construction and the number of observable nodes grows with the overall network size N ; whereas *ii*) in [36] the number of monitored nodes is held fixed (and, hence, the fraction of observable nodes vanishes in the limit of large N), the graph of the monitored nodes is left arbitrary, and the unobserved component continues to obey an Erdős-Rényi model. The present work focuses on the former model¹. It is therefore necessary to explain clearly why the present work constitutes a significant progress in the context of local tomography over diffusion networks, in comparison to [28].

3.3. Main Advances. In this work we consider the same setting adopted in [28], except for a slightly more restrictive assumption on the class of combination matrices, which is summarized in Assumption 1 further ahead. These matrices, referred to as *regular diffusion matrices*, arise quite naturally when the nodes’ combination weights are collected into a (scaled, i.e., stable version of a) symmetric doubly-stochastic matrix, whose support graph must match the underlying graph of connections. It is important to remark that all the matrices considered in the examples of the aforementioned previous works, as well as the most typical combination matrices, satisfy automatically such an assumption. The key contributions here in relation to [28] are as follows:

— One first advance regards the regime of connectivity. Reference [28] addresses only the case that the network is sparsely connected, which means that the connection probability is allowed to vanish with N , but in a way that preserves network connectedness. In this work we are able to establish that consistent local tomography is possible also under the *dense* regime, which means that the connection probability is *not* vanishing. Our results are established in terms of a strong notion of consistency (referred to as *universal local structural consistency*), which will be formally introduced in Sec. 6. Moreover, the analysis will reveal that the key-property to prove this

¹Even if the machinery used to prove our results can be applied to the latter model as well, we deem it useful to focus on a single model, in order to make the exposition more organic and to convey better the main message of the work.

consistency result is the *statistical concentration* of node degrees.

— We advance also with respect to the results currently available under the sparse regime. More specifically, in [28] a consistency result is proved, for all sparsely connected networks, in terms of an *average* fraction of misclassified node pairs. In the present work we are able to strengthen significantly this consistency result for the subclass of sparsely connected networks whose node degrees fulfill a statistical concentration property. For these networks, we ascertain that universal local structural consistency holds. Using such stronger notion of consistency answers also the following important question (posed, and only partially answered in [28], where the answer was obtained under a certain *approximation* of independence): *does the fraction of mistakes scale properly with N ?*

— We are able to offer a rigorous proof that the connected and non-connected agent pairs can be recovered through some *universal* clustering algorithm. In particular, we propose a variant of the k -means algorithm that is shown to be asymptotically consistent.

— The third advance regards the topology inference algorithms. Under the full-observability setting, it can be relatively easy, for a given dynamical system, to retrieve the right matrix estimator that contains information about the underlying graph. The three matrix estimators in Sec. 2 (i.e., R_0 , R_0^{-1} , or $R_1 R_0^{-1}$) constitute examples of how to manage this aspect in traditional graph learning models. On one hand, the matrix estimators available in the full-observability setting might orient the choice of a matrix estimator for the partial observability setting. For example, one can replace the Granger estimator with a version that considers only the subnetwork of observed measurements. This choice is widely adopted in causal inference from time series (when one neglects the existence of latent components), and has been adopted, e.g., in [28] and [36]. On the other hand, there is in principle no reason why the best solution to the partial observability setting is obtained by mimicking one matrix estimator that is good for the full observability setting. This concept is put forth in the present work, where, exploiting novel analytical methods to characterize the graph learning errors in terms of powers of the combination matrix, we are able to construct and examine different matrix estimators. In particular we will consider, along with the Granger estimator, two other matrix estimators, namely, the *one-lag correlation matrix* and the *correlation matrix between the residuals* (i.e., difference between subsequent time samples). First, we will be able to show that all the three estimators are structurally consistent. Then, we will show by numerical simulations that the Granger estimator can be outperformed, which confirms the hypothesis that what is good under full observability

might not be the best option to use under partial observability.

The bottom line of the novel results presented in this work is that the *fortunate coupling between the Erdős-Rényi model and the regular diffusion matrices renders the problem of topology inference a local problem*. Moreover, the analysis will reveal that, contrary to a widespread belief, sparsity is not necessarily the key-enabler for structural consistency under partial observability. Instead, the main enabling feature will be seen to be the error concentration induced by the aforementioned coupling.

Preliminary results related to this work are presented in the short conference articles [24, 25]. This work advances significantly w.r.t. [24, 25] as regards several aspects, including: detailed analysis of the graph concentration properties and their fundamental relationship with consistent learning; detailed analysis of local and/or universal consistency and their relationship with practical clustering algorithms; accurate characterization of a class of consistent matrix estimators; new mathematical results with rigorous proofs; numerical experiments.

3.4. Outline. The article is organized as follows. Section 4 introduces the dynamical system considered in this work, which encodes the relationships between the output measurements and the network topology. In Sec. 5 we describe the random model used for the graph, we present useful *statistical concentration* results that are critical for our treatment, and we introduce the *partial observation* setting. We remark that adopting a statistical approach is key to address the *large-scale* setting, since a *random* graph enables an asymptotic study of the thermodynamic behavior of the system as the network size grows. Our achievability results will be indeed established in a precise statistical sense, by showing that the estimated graph converges with high probability to the true graph. Following these lines, Sec. 6 introduces rigorous notions of consistency, and fundamental concepts such as margins, identifiability gap and bias, which are the building blocks to characterize in a precise statistical sense the limiting behavior of the inferential procedure. In relation to the concept of *universal* consistency, we prove the existence of a clustering algorithm that enables universal (i.e., fully data-driven) recovery of the true topology. In Sec. 7 we propose three matrix estimators, whose universal consistency is established in Sec. 8. Finally, Sec. 9 collects some examples aimed at illustrating the theoretical results.

Notation. We use boldface letters to denote random variables, and normal font letters for their realizations. Matrices are denoted by capital letters, and vectors by small letters. This convention can be occasionally violated, for example, the total number of network nodes is denoted by N .

The symbol $\xrightarrow{\text{P}}$ denotes convergence in probability as $N \rightarrow \infty$. When we say that an event occurs “w.h.p.” we mean that it occurs “with high probability” as $N \rightarrow \infty$.

Sets and events are denoted by upper-case calligraphic letters, whereas the corresponding normal font letter will denote the set cardinality. For example, the cardinality of \mathcal{S} is S . The complement of \mathcal{S} is denoted by \mathcal{S}' .

For a $K \times K$ matrix Z , the submatrix spanning the rows of Z indexed by set $\mathcal{S} \subseteq \{1, 2, \dots, K\}$ and the columns indexed by set $\mathcal{T} \subseteq \{1, 2, \dots, K\}$, is denoted by $Z_{\mathcal{S}\mathcal{T}}$, or alternatively by $[Z]_{\mathcal{S}\mathcal{T}}$. When $\mathcal{S} = \mathcal{T}$, the submatrix $Z_{\mathcal{S}\mathcal{T}}$ is abbreviated as $Z_{\mathcal{S}}$. Moreover, in the indexing of the submatrix we keep the index set of the original matrix. For example, if $\mathcal{S} = \{2, 3\}$ and $\mathcal{T} = \{2, 4, 5\}$, the submatrix $M = Z_{\mathcal{S}\mathcal{T}}$ is a 2×3 matrix, indexed as follows:

$$(3.1) \quad M = \begin{pmatrix} z_{22} & z_{24} & z_{25} \\ z_{32} & z_{34} & z_{35} \end{pmatrix} = \begin{pmatrix} m_{22} & m_{24} & m_{25} \\ m_{32} & m_{34} & m_{35} \end{pmatrix}.$$

The symbol \log denotes the natural logarithm.

4. Dynamical Graph System. Let $\mathbf{y}_i(n)$ be the output measurement produced by node i at time n . Likewise, let $\mathbf{x}_i(n)$ be the input source (e.g., streaming data or noise) exciting node i at time n . The random variables $\mathbf{x}_i(n)$ have zero mean and unit variance, and are independent and identically distributed (i.i.d.), both spatially (i.e., w.r.t. to index i) and temporally (i.e., w.r.t. to index n). It is convenient to stack the input and output variables, respectively, into the vectors:

$$(4.1) \quad \mathbf{x}_n = [\mathbf{x}_1(n), \mathbf{x}_2(n), \dots, \mathbf{x}_N(n)]^\top, \quad \mathbf{y}_n = [\mathbf{y}_1(n), \mathbf{y}_2(n), \dots, \mathbf{y}_N(n)]^\top.$$

The stochastic dynamical system considered in the present work is given by the following *network diffusion* process (a.k.a. first-order Vector AutoRegressive (VAR) model):

$$(4.2) \quad \boxed{\mathbf{y}_n = A \mathbf{y}_{n-1} + \sigma \mathbf{x}_n}$$

where A is some stable $N \times N$ matrix with nonnegative entries, and σ^2 is a variance factor. By rewriting (4.2) on an entrywise basis:

$$(4.3) \quad \mathbf{y}_i(n) = \sum_{\ell=1}^N a_{i\ell} \mathbf{y}_\ell(n-1) + \sigma \mathbf{x}_i(n),$$

we readily see that the support-graph of A reflects the connections among the network nodes. Indeed, Eq. (4.3) shows that, at time n , the output of

node i is updated by *combining* the outputs of other nodes from time $n-1$. In particular, node i scales the output of node ℓ by using a combination weight $a_{i\ell}$, which implies that the output of agent ℓ is *effectively used* by node i if, and only if $a_{i\ell} \neq 0$. After the combination step, the output measurement $\mathbf{y}_i(n)$ is adjusted by incorporating the streaming-source value, $\mathbf{x}_i(n)$, which is locally available at node i at current time n .

In our *partial observation* setting, only a subset of nodes can be probed: for each node i belonging to the subset of probed nodes, \mathcal{S} , a stream of n_{obs} measurements, $\mathbf{y}_i(1), \mathbf{y}_i(2), \dots, \mathbf{y}_i(n_{\text{obs}})$ is acquired. The learning task is to reconstruct the graph of interconnections corresponding to the combination (sub)matrix $A_{\mathcal{S}}$.

Formulations like the one in (4.2) arise naturally across application domains, e.g., in economics [31], in the variational characterization of nonlinear stochastic dynamical systems [32], or in distributed network processing applications where several useful strategies such as consensus [3, 8, 13] and diffusion [39] lead to data models of the form in (4.3).

5. Random Graph Model. In the following, we shall denote by \mathbf{G} the adjacency matrix of the network graph, whose entry \mathbf{g}_{ij} is equal to one if nodes i and j are connected, and is equal to zero otherwise. The bold notation is used because we deal with *random* graphs.

In this article we address the useful case where the network graph is generated according to the Erdős-Rényi *random graph* model, namely, an undirected graph whose edges are drawn, one independently from the other, through a sequence of Bernoulli experiments with identical success (i.e., connection) probability [6, 14]. In particular, the notation $\mathbf{G} \sim \mathcal{G}(N, p_N)$ will signify that the off-diagonal entries of the adjacency matrix \mathbf{G} originate from an Erdős-Rényi graph over N nodes, and with connection probability p_N . Accordingly, the variables \mathbf{g}_{ij} , for $i = 1, 2, \dots, N$ and $j > i$, are independent Bernoulli random variables with $\mathbb{P}[\mathbf{g}_{ij} = 1] = p_N$, and the matrix \mathbf{G} is symmetric. As it will be clear soon, the explicit dependence of the connection probability upon N will be critical to examine the evolution of random graphs in the thermodynamic limit of large N .

As one fundamental graph descriptor, in this work we use the *degree* of a node. The degree of node i is defined as:

$$(5.1) \quad \mathbf{d}_i = 1 + \sum_{\ell \neq i} \mathbf{g}_{i\ell} = 1 + \sum_{\ell \neq i} \mathbf{g}_{\ell i},$$

namely, the cardinality of the i -th node neighborhood (including i itself). In particular, we shall use the minimal and maximal degrees that are defined

as, respectively:

$$(5.2) \quad \mathbf{d}_{\min} \triangleq \min_{i=1,2,\dots,N} \mathbf{d}_i, \quad \mathbf{d}_{\max} \triangleq \max_{i=1,2,\dots,N} \mathbf{d}_i.$$

5.1. *Thermodynamic Limit of Random Graphs.* One meaningful (and classic) way to characterize the behavior of random graphs is to examine their thermodynamic limit as the network size goes to infinity. Such an asymptotic characterization is useful because it captures average behavior that emerges with high probability over large networks.

In examining the thermodynamic behavior of random graphs, the connection probability p_N is generally allowed to scale with N . This degree of freedom allows representing different types of asymptotic graph behavior. For example, recalling that the average number of neighbors over an Erdős-Rényi graph scales as Np_N , different graph evolutions can be obtained with different choices of p_N . For example, a constant p_N will let the number of neighbors grow linearly with N . In comparison, a p_N scaling as $(\log N)/N$ would correspond to a number of neighbors growing logarithmically with N . In summary, different limiting regimes are determined by the way the connection probability evolves with N . It is useful for our purposes to list briefly the main regimes that are of interest for the forthcoming treatment.

— *Connected regime.* In this work we focus on the regime where the graph is connected with high probability. This regime prescribes that the pairwise connection probability scales as [6, 14]:

$$(5.3) \quad p_N = \frac{\log N + c_N}{N}, \quad c_N \xrightarrow{N \rightarrow \infty} \infty.$$

— *Sparse (connected) regime.* The connected regime can be obtained also when the pairwise connection probability, p_N , vanishes as N gets large. In particular, we shall refer to this scenario as the *sparse* connected regime:

$$(5.4) \quad p_N \xrightarrow{N \rightarrow \infty} 0 \quad \text{under (5.3)} \quad [\text{Sparse connection regime}].$$

— *Dense regime.* We call *dense* the regime where the pairwise connection probability converges to a nonzero quantity, namely $p_N \rightarrow p > 0$.

The aforementioned taxonomy basically focuses on the concepts of connectedness and sparsity. These concepts have been advocated in previous works related to topology inference with partial observations, and, in particular, some useful structural consistency results have been proved under the sparse (connected) regime.

One essential element of novelty in our analysis is exploiting a different feature, namely, the *concentration* of graph degrees. We wish to avoid confusion here: the term “concentration” does *not* refer to the number of node

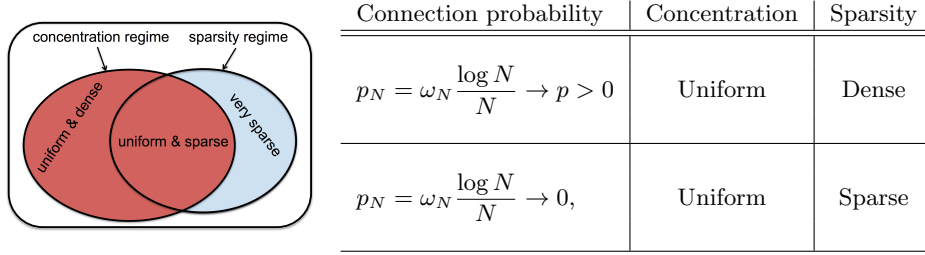


FIG 1. Useful taxonomy to illustrate the relationships between concentration and sparsity over a connected network. The sequence ω_N goes to infinity as $N \rightarrow \infty$.

connections. Instead, the concept of concentration is borrowed from a common terminology in statistics, which is used to refer to statistical quantities that concentrate around some (deterministic) value as $N \rightarrow \infty$ [7]. In particular, we will focus our attention on the *uniform concentration properties of the minimal and maximal degrees of random graphs*.

— *Uniform concentration regime*. The uniform concentration regime is enabled by choosing the following pairwise connection probability:

$$(5.5) \quad p_N = \omega_N \frac{\log N}{N} \xrightarrow{N \rightarrow \infty} p, \quad \omega_N \xrightarrow{N \rightarrow \infty} \infty,$$

which is tantamount to assuming that (5.3) holds true with the sequence c_N growing faster than $\log N$. Under this regime, the minimal and the maximal degrees of the graph both concentrate asymptotically around the expected degree $(1 + (N - 1)p_N \sim Np_N)$, in the following precise sense:

$$(5.6) \quad \boxed{\frac{\mathbf{d}_{\min}}{Np_N} \xrightarrow{p} 1, \quad \frac{\mathbf{d}_{\max}}{Np_N} \xrightarrow{p} 1, \quad [\text{Uniform concentration}]}$$

The physical meaning of (A.10) is that both the minimal and the maximal degrees scale, asymptotically with N , as the expected degree. Indeed, Eq. (A.10) can be restated as: $\mathbf{d}_{\min} \sim Np_N + f_N$ and $\mathbf{d}_{\max} \sim Np_N + g_N$, where f_N and g_N are sequences that are asymptotically dominated by Np_N .

Figure 1 summarizes the sparsity/concentration taxonomy arising from the previous arguments. We are now ready to extract from the above taxonomy the elements that are relevant to the forthcoming treatment:

1. Comparing (5.5) against (5.3), we see that the regime of concentration does *not* include all classes of connected Erdős-Rényi graphs. In fact, while in (5.3) c_N is any arbitrary divergent sequence (e.g., we can have $c_N = \log \log N$), according to (5.5) the sequence c_N should grow

with N more than logarithmically. The regime where the graph is connected, whereas (5.5) is not fulfilled, will be referred to as the *very sparse* regime.

2. According to (5.5), the regime of concentration can be either sparse or dense. In particular, the regime is dense when $p > 0$, and is sparse when $p = 0$.

After having introduced the necessary details for the generation of the whole network, we are ready to introduce the formal model for partial observations.

DEFINITION 1 (Partial observation setting). *In this work we adopt the partial observation setting that has been introduced in [28]: the entire network graph is generated according to the Erdős-Rényi model, and the subnetwork of observable measurements, \mathcal{S} , has a cardinality S scaling as:*

$$(5.7) \quad \frac{S}{N} \xrightarrow{N \rightarrow \infty} \xi \in (0, 1),$$

which means that ξ is the (asymptotic) fraction of monitored nodes. Since ξ is strictly less than one, condition (5.7) conforms to a partial observation setting.

5.2. From Graphs to Combination Matrices. We start by introducing a useful class of combination matrices.

ASSUMPTION 1 (Regular diffusion matrices). *We assume here that the combination matrix \mathbf{A} is symmetric and that:*

$$(5.8) \quad \boxed{\sum_{\ell=1}^N \mathbf{a}_{i\ell} = \rho, \quad \frac{\kappa}{\mathbf{d}_{\max}} \mathbf{g}_{ij} \leq \mathbf{a}_{ij} \leq \frac{\kappa}{\mathbf{d}_{\min}} \mathbf{g}_{ij} \quad \forall i \neq j}$$

for some parameters ρ and κ , with $0 < \rho < 1$ and $0 < \kappa \leq \rho$. □

For the sake of concreteness, in the following we shall refer to combination matrices obeying the aforementioned assumption as *regular diffusion matrices* with parameters ρ and κ . We must remark that the most common combination matrices encountered in the literature automatically satisfy Assumption 1. For example, some popular choices are the Laplacian and the Metropolis rules reported below, which arise naturally in many applications, for instance, they are one fundamental ingredient of *adaptive* networks [27].

The matrix entries corresponding to these combination rules are defined as follows. For $i \neq j$:

$$(5.9) \quad \mathbf{a}_{ij} = \rho \lambda \frac{\mathbf{g}_{ij}}{\mathbf{d}_{\max}}, \quad [\text{Laplacian rule}]$$

$$(5.10) \quad \mathbf{a}_{ij} = \rho \frac{\mathbf{g}_{ij}}{\max\{\mathbf{d}_i, \mathbf{d}_j\}}, \quad [\text{Metropolis rule}]$$

whereas the self-weights are determined by the leftmost condition in (5.8), yielding $\mathbf{a}_{ii} = \rho - \sum_{\ell \neq i} \mathbf{a}_{i\ell}$. For the Laplacian rule, the parameter λ fulfills the inequalities $0 < \lambda \leq 1$.

6. Consistent Graph Learning. In order to ascertain whether or not it is possible to discriminate interacting (i.e., connected) agents from non-interacting agents, via observation of their output measurements, we now introduce the concept of margins and identifiability gap.

DEFINITION 2 (Margins). *Let $\widehat{\mathbf{A}}_{\mathcal{S}}$ be a certain estimated combination matrix, corresponding to the subset \mathcal{S} . The lower and upper margins corresponding to the disconnected pairs are defined as, respectively²:*

$$(6.1) \quad \underline{\delta}_N \triangleq \min_{\substack{i,j \in \mathcal{S}: \mathbf{a}_{ij}=0 \\ i \neq j}} \widehat{\mathbf{a}}_{ij}, \quad \overline{\delta}_N \triangleq \max_{\substack{i,j \in \mathcal{S}: \mathbf{a}_{ij}=0 \\ i \neq j}} \widehat{\mathbf{a}}_{ij}.$$

Likewise, the lower and upper margins corresponding to the connected pairs are defined as, respectively:

$$(6.2) \quad \underline{\Delta}_N \triangleq \min_{\substack{i,j \in \mathcal{S}: \mathbf{a}_{ij}>0 \\ i \neq j}} \widehat{\mathbf{a}}_{ij}, \quad \overline{\Delta}_N \triangleq \max_{\substack{i,j \in \mathcal{S}: \mathbf{a}_{ij}>0 \\ i \neq j}} \widehat{\mathbf{a}}_{ij}.$$

□

The aforementioned margins are useful to examine the achievability of structural consistency for an estimator $\widehat{\mathbf{A}}_{\mathcal{S}}$ — see Fig. 2 for an illustration — and lead to the concept of *identifiability gap*.

DEFINITION 3 (Local structural consistency). *Let $\widehat{\mathbf{A}}_{\mathcal{S}}$ be an estimated combination matrix. If there exists a sequence s_N , a real value η , and a strictly positive value Γ , such that, for all $\epsilon > 0$:*

$$(6.3) \quad \boxed{\begin{array}{l} s_N \overline{\delta}_N < \eta + \epsilon \quad \text{w.h.p.}, \\ s_N \underline{\Delta}_N > \eta + \Gamma - \epsilon \quad \text{w.h.p.} \end{array}}$$

²The definitions in (6.1) and (6.2) are void if the nodes in \mathcal{S} are all connected or all disconnected, respectively. Since, under the Erdős-Rényi model, these events are irrelevant as $N \rightarrow \infty$, for these singular cases we can formally assign arbitrary values to the margins.

we say that $\widehat{\mathbf{A}}_{\mathcal{S}}$ achieves local structural consistency, with a bias at most equal to η , an identifiability gap at least equal to Γ , and with a scaling sequence s_N . \square

REMARK 1 (Locality). We use the qualification “local” to remark that the structure of the subnetwork \mathcal{S} must be inferred from observations gathered *locally* in \mathcal{S} , even if the nodes of \mathcal{S} undergo the influence of many other nodes belonging to the larger embedding network, $\mathcal{N} \supset \mathcal{S}$. \square

REMARK 2 (Identifiability gap). The condition $s_N \bar{\delta}_N < \eta + \epsilon$ w.h.p. means that the *maximum* entry of $s_N \widehat{\mathbf{A}}_{\mathcal{S}}$ taken over the *disconnected* pairs essentially does not exceed η . Likewise, the condition $s_N \underline{\Delta}_N > \eta + \Gamma - \epsilon$ w.h.p. means that the *minimum* entry of $s_N \widehat{\mathbf{A}}_{\mathcal{S}}$ taken over the *connected* pairs essentially stays above the value $\eta + \Gamma > \eta$. Combining these two relationships, we conclude that the estimated matrix entries corresponding to connected node pairs stand clearly separated from the entries corresponding to disconnected node pairs. The minimum amount of separation is quantified by the gap, Γ . \square

REMARK 3 (Bias). For the *true* combination matrix, the entries corresponding to disconnected pairs are zero. In contrast, Eq. (6.3) reveals that the scaled entries for disconnected pairs can be close to η , which results therefore in a *bias*. However, and remarkably, *this bias does not constitute a problem for consistent classification of connected/non-connected nodes*, namely, the bias does not affect in any manner identifiability. \square

The notion of structural consistency implies the existence of a threshold, comprised between η and $\eta + \Gamma$, which correctly separates (in the limit of large N) the entries of the matrix estimator, in such a way that the entries corresponding to connected pairs lie above the threshold, whereas the entries corresponding to disconnected pairs lie below the threshold.

However, an accurate determination of the separation threshold requires some prior knowledge of the monitored system. For instance, to set a detection threshold one needs to know the scaling sequence s_N . In the problems dealt with in this work we will see that $s_N = Np_N$, where Np_N represents the average number of neighbors in the network, and in several practical applications this number is unknown.

As a result, the threshold setting might be a critical issue, and it would be highly desirable to have a *universal* (i.e., blind and nonparametric) method to set the threshold. For example, it would be highly desirable to determine

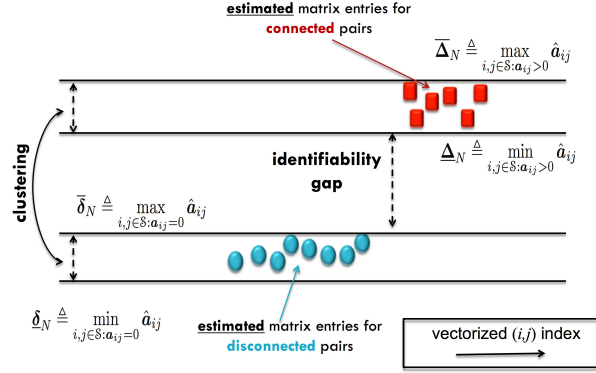


FIG 2. Emergence of the identifiability gap.

a separation threshold using machine learning tools such as a standard clustering algorithm (e.g., a k -means clustering with $k = 2$). It is therefore useful to strengthen the notion of structural consistency so as to incorporate the aforementioned requirement of universality.

DEFINITION 4 (Universal local structural consistency). *Let $\widehat{\mathbf{A}}_S$ be an estimated combination matrix. If there exists a sequence s_N , a real value η , and a strictly positive value Γ , such that:*

$$(6.4) \quad \begin{array}{cc} s_N \underline{\delta}_N \xrightarrow{p} \eta, & s_N \underline{\Delta}_N \xrightarrow{p} \eta + \Gamma \\ s_N \overline{\delta}_N \xrightarrow{p} \eta, & s_N \overline{\Delta}_N \xrightarrow{p} \eta + \Gamma \end{array}$$

we say that $\widehat{\mathbf{A}}_S$ achieves uniform local structural consistency, with a bias η , an identifiability gap Γ , and with a scaling sequence s_N . \square

REMARK 4 (Clustering). According to the notion of *universal* structural consistency, the pair of (scaled) lower margins, $s_N \underline{\delta}_N$ and $s_N \overline{\delta}_N$, converge to one and the same value, η , which implies that *all the entries of $s_N \widehat{\mathbf{A}}_S$ corresponding to disconnected pairs* are sandwiched between these margins — see Fig. 2. A similar behavior is observed for the scaled entries over the connected pairs, which converge altogether to $\eta + \Gamma$ since they are sandwiched between $s_N \underline{\Delta}_N$ and $s_N \overline{\Delta}_N$. In summary, we conclude that the connected and disconnected agent pairs *cluster into well-separated classes* that can be identified, e.g., by means of a universal clustering algorithm. \square

REMARK 5 (Scale-irrelevance). The definition of identifiability and consistency do not clarify what would be the right value for the identifiability

gap. For example, assume that a certain estimator $\widehat{\mathbf{A}}_S$ leads to a gap Γ . If we now construct another estimator $c\widehat{\mathbf{A}}_S$, i.e., if we scale $\widehat{\mathbf{A}}_S$ by some constant c , then the gap becomes $c\Gamma$. This would imply that choosing an arbitrarily large value for c would lead to an arbitrarily large gap, what does this mean?

This observation provides an opportunity to clarify the meaning of the identifiability gap. The concept behind identifiability is that there exists a strictly positive Γ that allows separating the two sets of connected and disconnected agent pairs. Asymptotically, the existence of a strictly positive Γ enables successful discrimination. Moreover, for finite network sizes, the value itself of the gap is not informative about the performance achievable by a classifier that operates on the entries of the estimated matrix. What really determines the classifier performance is the *variance of the entries relative to the gap value*. In other words, the performance of the classifier is determined by how much the matrix entries spread around their limiting values. A high spread makes classification more difficult, whereas a low spread facilitates identification of the correct network structure. For similar reasons, clustering algorithms are clearly unaffected by changes in scale, while they are sensitive to the spread of the entries within each individual cluster. Characterizing the spread requires a higher-order analysis that goes beyond the scope of this work. \square

6.1. *A Consistent Clustering Algorithm.* The definition of universal local structural consistency implies that the disconnected node pairs cluster around η , whereas the connected node pairs cluster around the higher value $\eta + \Gamma$. Accordingly, for sufficiently large N , there is no doubt that any reasonable clustering algorithm will be able to identify properly these two clusters. For example, a correct *asymptotic* guess of the true clusters (i.e., of the true graph) can be obtained by simply choosing an intermediate threshold between the maximum and the minimum matrix entries.

On the other hand, since in practice we work with *finite* network sizes, a number of non-ideal effects could appear, and the non-perfect localization of the clusters could affect the inference performance. For these reasons, we start by focusing on a popular and general-purpose clustering algorithm, namely, the k -means algorithm (in our case, we know that $k = 2$), because it typically offers good performance under many operational conditions. However, and somehow paradoxically, while the k -means works properly for finite network sizes, it is not obvious that it should be *asymptotically* consistent. This is because the k -means might suffer when dealing with clusters of very different sizes. Since in our model it is actually permitted that, for large N , one cluster can dominate the other one (for instance, when $p_N \rightarrow 0$, the

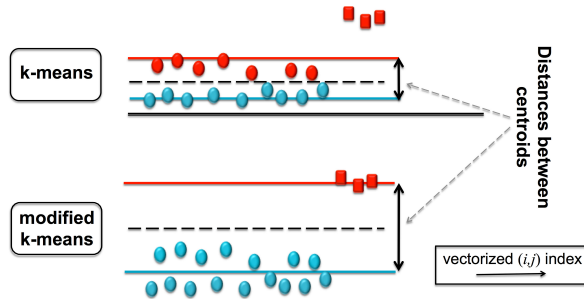


FIG 3. Visual comparison between the k -means algorithm and the modified k -means algorithm proposed in this work, for the case of unbalanced clusters. The true clusters are identified by different symbols (circle vs. square). The clusters produced by the algorithms are identified by different colors (blue vs. red).

cluster of disconnected nodes becomes predominant), we are not guaranteed that the k -means algorithm works properly as $N \rightarrow \infty$.

In order to circumvent this problem, we propose a slight modification of the k -means algorithm that is specifically tailored to the universal local structural consistency property. Preliminarily, let v be the $L \times 1$ vector to be clustered, with entries that have been arranged in ascending order. The k -means algorithm, with $k = 2$, attempts to minimize the following cost function:

$$(6.5) \quad \sum_{j \in \mathcal{C}_0} (v_j - c_0)^2 + \sum_{j \in \mathcal{C}_1} (v_j - c_1)^2,$$

over all possible clusters \mathcal{C}_0 and \mathcal{C}_1 , with c_0 and c_1 being the cluster centroids. It is useful to recall that the minimum of the cost function must fulfill the following necessary condition: the midpoint between the two centroids is a threshold that separates the two clusters. In our one-dimensional case, with $k = 2$, this property implies that it suffices to consider only the cluster configurations $\mathcal{C}_0 = \{1, 2, \dots, j\}$ and $\mathcal{C}_1 = \{j + 1, j + 2, \dots, L\}$, for $j \in \{1, 2, \dots, L - 1\}$. (Obviously, if two points, say v_i and v_{i+1} , are coincident, considering their possible permutations is pointless). Accordingly, we see that any possible partition is identified by an index j .

Let us now describe the modified k -means algorithm we propose. First, the algorithm enumerates all admissible clusters through an index j spanning the set $\{1, 2, \dots, L - 1\}$. The set of indices fulfilling the necessary condition of k -means are collected in the set $\mathcal{A} = \{j_1, j_2, \dots\}$. At this stage, the classic k -means would simply select, among these admissible points, the one ensuring the minimum cost. We modify this rule by selecting the index

$j^* \in \mathcal{A}$ that maximizes the distance between the clusters' centroids, namely, $j^* = \operatorname{argmin}_{j \in \mathcal{A}} [c_1(j) - c_0(j)]$, with $c_0(j)$ and $c_1(j)$ being the centroids corresponding to the clusters identified by index j . With this modified rule, we want to *i*) retain the good behavior exhibited by k -means in typical situations; and *ii*) guarantee that the algorithm provides the correct answer as $N \rightarrow \infty$. Point *i*) will be confirmed by the numerical experiments in Sec. 9.

Point *ii*) can be proved as follows. For large N , the true clusters become almost perfectly localized, and, hence, two centroids belonging to the true clusters match the necessary condition (lowermost panel in Fig. 3). However, if the sizes of the true clusters are very different, the effect of the smallest ensemble (squares) could be asymptotically negligible, resulting into the configuration illustrated in the uppermost panel of Fig. 3. Here the two centroids estimated by the k -means algorithm are both located within the largest ensemble (circles), leading to a wrong partitioning. In contrast, the modified k -means would guess the right configuration, because such configuration maximizes the distance between the centroids, as is clear from the comparison between the two panels in Fig. 3.

7. Proposed Matrix Estimators. We now introduce the three estimators examined in this work.

7.1. *Granger Estimator.* For the model in (4.2), it is straightforward to obtain the following well-known relationship:

$$(7.1) \quad \mathbf{A} = \mathbf{R}_1 \mathbf{R}_0^{-1},$$

a quantity that is also referred to as the best one-step predictor or Granger estimator [17, 21]. Under the partial observability setting, it is tempting to adapt the structure in (7.1) by considering only the observable subnet \mathcal{S} , and by neglecting the effect of the latent nodes, yielding [28, 36]:

$$(7.2) \quad \widehat{\mathbf{A}}_{\mathcal{S}} = [\mathbf{R}_1]_{\mathcal{S}} ([\mathbf{R}_0]_{\mathcal{S}})^{-1}.$$

In order to evaluate the accuracy of this matrix estimator, we introduce the error matrix $\mathbf{E} \triangleq \widehat{\mathbf{A}}_{\mathcal{S}} - \mathbf{A}_{\mathcal{S}}$. In [28] it is shown that such error matrix admits the following compact representation (we recall that \mathcal{S}' denotes the subset of unobserved nodes):

$$(7.3) \quad \mathbf{E}^{(\text{Gra})} = \mathbf{A}_{\mathcal{S}\mathcal{S}'} \mathbf{H} [\mathbf{A}^2]_{\mathcal{S}'\mathcal{S}},$$

where

$$(7.4) \quad \mathbf{H} = (\mathbf{I}_{N-K} - \mathbf{C})^{-1}, \quad \text{with } \mathbf{C} \triangleq [\mathbf{A}^2]_{\mathcal{S}'\mathcal{S}}.$$

For later use, it is also useful to write (7.3) on an entrywise basis:

$$(7.5) \quad \mathbf{e}_{ij}^{(\text{Gra})} = \sum_{\ell, m \in \mathcal{S}'} \mathbf{a}_{i\ell} \mathbf{h}_{\ell m} \mathbf{a}_{mj}^{(2)}, \quad i, j \in \mathcal{S}.$$

7.2. One-Lag Correlation Estimator. In this section we use the one-lag correlation matrix as estimator for the combination matrix. The reason behind³ such choice is the following series expansion of the one-lag correlation matrix:

$$(7.6) \quad \mathbf{R}_1 = \mathbf{A}\mathbf{R}_0 = \sigma^2 \mathbf{A}(\mathbf{I}_N - \mathbf{A}^2)^{-1} = \sigma^2 (\mathbf{A} + \mathbf{A}^3 + \mathbf{A}^5 + \dots)$$

which when applied only to the submatrix corresponding to \mathcal{S} , yields:

$$(7.7) \quad \widehat{\mathbf{A}}_{\mathcal{S}}^{(1\text{-lag})} = [\mathbf{R}_1]_{\mathcal{S}} = \sigma^2 \mathbf{A}_{\mathcal{S}} + \sigma^2 ([\mathbf{A}^3]_{\mathcal{S}} + [\mathbf{A}^5]_{\mathcal{S}} + \dots).$$

Accordingly, the series of odd powers in (7.7) can be interpreted as an error term, yielding:

$$(7.8) \quad \mathbf{E}^{(1\text{-lag})} = \widehat{\mathbf{A}}_{\mathcal{S}}^{(1\text{-lag})} - \sigma^2 \mathbf{A}_{\mathcal{S}} = \sigma^2 \sum_{h=1}^{\infty} [\mathbf{A}^{2h+1}]_{\mathcal{S}},$$

or, on an entrywise basis, for all $i, j \in \mathcal{S}$:

$$(7.9) \quad \widehat{\mathbf{a}}_{ij}^{(1\text{-lag})} = \sigma^2 \mathbf{a}_{ij} + \mathbf{e}_{ij}^{(1\text{-lag})}, \quad \mathbf{e}_{ij}^{(1\text{-lag})} = \sigma^2 \sum_{h=1}^{\infty} \mathbf{a}_{ij}^{(2h+1)}.$$

7.3. Residual Estimator. Let us introduce the residual vector that computes the (scaled) difference between consecutive time samples:

$$(7.10) \quad \mathbf{r}_n \triangleq \frac{\mathbf{y}_n - \mathbf{y}_{n-1}}{\sqrt{2}}.$$

We have clearly $\mathbb{E}[\mathbf{r}_n \mathbf{r}_n^{\top}] = \mathbf{R}_0 - \mathbf{R}_1 = \sigma^2 (\mathbf{I}_N + \mathbf{A})^{-1}$. Accordingly, it makes sense to introduce the following estimator:

$$(7.11) \quad \begin{aligned} \widehat{\mathbf{A}}_{\mathcal{S}}^{(\text{res})} &= [\mathbf{R}_1]_{\mathcal{S}} - [\mathbf{R}_0]_{\mathcal{S}} = -\sigma^2 [(\mathbf{I}_N + \mathbf{A})^{-1}]_{\mathcal{S}} \\ &= \sigma^2 \mathbf{A}_{\mathcal{S}} + \sigma^2 (-\mathbf{I}_{\mathcal{S}} - [\mathbf{A}^2]_{\mathcal{S}} + [\mathbf{A}^3]_{\mathcal{S}} + \dots), \end{aligned}$$

³When σ^2 is known, the relationship between $\mathbf{R}_1 = \sigma^2 \mathbf{A}(\mathbf{I}_N - \mathbf{A}^2)^{-1}$ and \mathbf{A} is invertible under the full observability regime. This can be easily shown by resorting to the spectral decomposition of \mathbf{R}_1/σ^2 and \mathbf{A} (which share the same eigenvectors), and by finding the eigenvalues of \mathbf{A} from those of \mathbf{R}_1/σ^2 ; this inversion operation can be successfully realized because \mathbf{A} is symmetric and has spectral radius less than one. However, we remark that σ^2 is assumed unknown and, more importantly, that we work under a partial observability regime, and, hence, the aforementioned inversion procedure does not apply.

Estimator	Error bias η	Identifiability gap Γ
Granger: $[\mathbf{R}_1]_{\mathcal{S}}([\mathbf{R}_0]_{\mathcal{S}})^{-1}$	$\kappa^2 p \frac{(2\rho - \kappa)(1 - \xi)}{1 - (\rho^2 - 2\rho\kappa\xi + \kappa^2\xi)}$	κ
one-lag: $[\mathbf{R}_1]_{\mathcal{S}}$	$\sigma^2 \kappa^2 p \frac{\rho + \rho(\rho - \kappa)^2 + 2(\rho - \kappa)}{(1 - \rho^2)(1 - (\rho - \kappa)^2)^2}$	$\frac{1 + (\rho - \kappa)^2}{(1 - (\rho - \kappa)^2)^2} \times \sigma^2 \kappa$
residual: $[\mathbf{R}_1]_{\mathcal{S}} - [\mathbf{R}_0]_{\mathcal{S}}$	$-\frac{\sigma^2 \kappa^2 p}{(1 + \rho)(1 + \rho - \kappa)^2}$	$\frac{\sigma^2 \kappa}{(1 + \rho - \kappa)^2}$

TABLE 1

Theorem 1: Biases and gaps of the three estimators listed in the leftmost column. For all cases, the scaling sequence is $s_N = Np_N$.

which gives rise implicitly to the error matrix:

$$(7.12) \quad \mathbf{E}^{(\text{res})} = -\sigma^2 I_{\mathcal{S}} + \sigma^2 \sum_{h=1}^{\infty} ([\mathbf{A}^{2h+1}]_{\mathcal{S}} - [\mathbf{A}^{2h}]_{\mathcal{S}}).$$

This means that, for all $i, j \in \mathcal{S}$, with $i \neq j$:

$$(7.13) \quad \hat{\mathbf{a}}_{ij}^{(\text{res})} = \sigma^2 \mathbf{a}_{ij} + \mathbf{e}_{ij}^{(\text{res})}, \quad \mathbf{e}_{ij}^{(\text{res})} = \sigma^2 \sum_{h=1}^{\infty} \left(\mathbf{a}_{ij}^{(2h+1)} - \mathbf{a}_{ij}^{(2h)} \right).$$

Before ending this section, we would like to remark that the errors in (7.8) and (7.12) are not defined with respect to the submatrix $\mathbf{A}_{\mathcal{S}}$, but with respect to its *scaled* version, $\sigma^2 \mathbf{A}_{\mathcal{S}}$. In other words, an error matrix identically equal to zero would not correspond to recovering $\mathbf{A}_{\mathcal{S}}$, but $\sigma^2 \mathbf{A}_{\mathcal{S}}$. If we were instead interested in estimating the combination matrix, the scaling factor would introduce an undesired bias in the estimation of $\mathbf{A}_{\mathcal{S}}$. However, the objective of structure learning is not to estimate the combination matrix, but rather to discriminate connected node pairs from disconnected ones. For this reason, the scaling factor is irrelevant.

REMARK 6. *One essential ingredient for the proof of Theorem 1 further ahead is characterizing the convergence properties of the error series in (7.5), (7.9) and (7.13). The different behavior of these series can give rise to different performance of the graph learners. For example, comparing (7.8) against (7.12), we see that, due to the subtraction of the correlation matrix \mathbf{R}_0 , the error of the residual estimator takes the structure of an alternating*

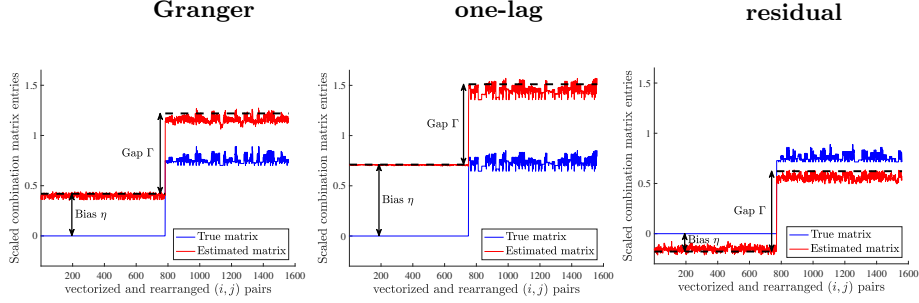


FIG 4. *Graphical illustration of Theorem 1. The three panels refer to the matrix estimators considered in the theorem. In each panel, the entries of the true matrix \mathbf{A}_S are vectorized following column-major ordering, and the (vectorized) (i, j) pairs are rearranged in such a way that the zero entries (blue markers) appear before the nonzero entries (red markers). The same ordering used for the true matrix is applied to the entries of the estimated matrix, $\hat{\mathbf{A}}_S$, and entries that correspond to truly disconnected pairs are displayed in black, whereas entries that correspond to truly connected pairs are displayed in green. Broken lines display the theoretical values: the lowermost line refers to the error gap, η , and the uppermost line refers to the quantity $\eta + \Gamma$, where Γ is the identifiability gap.*

series. This feature might be useful to reduce the error and, hence, to improve the performance of the graph learner. We will explore this aspect in Sec. 9.

8. Achievability of Universal Local Structural Consistency. The following theorem establishes the fundamental consistency properties of the estimators presented in Sec. 7.

THEOREM 1 (Universal local structural consistency). *Let \mathbf{A} be a regular diffusion matrix with parameters ρ and κ , with the network graph drawn according to an Erdős-Rényi random graph model $\mathcal{G}(N, p_N)$ where the fraction of observable nodes, S/N , converges to some nonzero value ξ .*

Then, under the uniform concentration regime where:

$$(8.1) \quad p_N = \omega_N \frac{\log N}{N} \rightarrow p, \quad \text{with } \omega_N \rightarrow \infty,$$

the Granger, the one-lag, and the residual estimators achieve universal local structural consistency, with a scaling sequence $s_N = Np_N$, and with the error biases and identifiability gaps listed in Table 1.

PROOF. The proof of the theorem is provided in Appendix C, and relies heavily on a number of auxiliary lemmas and theorems proved in the appendices. In particular, the core of the proof is the following. First, Theorems 2

and 3 in Appendix B construct *uniform* (w.r.t. N) bounds on the entries of the combination matrix and related matrices that are useful to characterize the error matrices associated to the three matrix estimators listed in Table 1. Then, thanks to these uniform bounds, and exploiting the asymptotic concentration property of the maximal and minimal degrees, it is possible to prove the convergence of the matrix series relevant for the computation of the errors, namely, Eqs. (7.5), (7.9) and (7.13). These convergence properties will be useful to compute the bias and the identifiability gaps listed in Table 1. \square

The main message conveyed by Theorem 1 is illustrated in Fig. 4, where we depict: *i*) the entries of the true combination matrix (disconnected pairs are displayed in blue, connected pairs are displayed in red), vectorized and ordered as shown in the figure, and magnified by Np_N ; and *ii*) the entries of the estimated combination matrix, magnified by Np_N , vectorized and ordered with the same ordering used for the true combination matrix. The three panels refer to the three estimators considered in this work, as detailed in the panel titles. The essential features illustrated in Sec. 6 are clearly visible in Fig. 4. First, we can appreciate the emergence of the gap Γ and of the bias η , which, remarkably, match well the theoretical predictions summarized in Table 1, as indicated by the broken lines (theoretical limiting values). It is also seen how the bias does not affect separability between the groups of connected and disconnected agents. Second, we see how the entries are clustered around the values predicted by the theorem. Moreover, we remark that the performance of the three learning algorithms cannot be anticipated from the claim of Theorem 1. Referring to Fig. 4, the observed values of biases and gaps do not contain information useful to compare the estimators against each other. What plays a role in their performance is the spread of the matrix entries around their limiting values. In the particular example shown in Fig. 4, the one-lag estimator seems to offer a better concentration (i.e., a lower spread) than the residual estimator, which seems in turn to exhibit a lower spread as compared to the Granger estimator.

Another useful conclusion stemming from Theorem 1 pertains to the dependence of the main quantities in Table 1 on the system parameters. We start by examining the identifiability gap. First, we have chosen for all three estimator the same scaling sequence, namely, $s_N = Np_N$. With this choice, we see that the gap of the Granger estimator is equal to the bounding constant κ that characterizes the regular diffusion matrix (5.8).

Let us now focus on the gaps pertaining to the one-lag and to the residual estimators. Both of them exhibit two main differences with respect to the

Granger estimator. First, they depend also on the variance of the input process, σ^2 . This behavior should be expected, since in the Granger estimator the one-lag correlation matrix multiplies the inverse of the correlation matrix, and, hence, the effect of σ^2 disappears. In contrast, the one-lag and the residual estimators do not cancel this effect. Second, when $\kappa \neq \rho$ (a condition that occurs, for instance, for the Laplacian rule), the term $\sigma^2\kappa$ multiplies a factor that is a function of $\rho - \kappa$. This factor is greater than one for the one-lag estimator, whereas it is smaller than one for the residual estimator. However, due to scale-irrelevance, we see that, in the absence of any information about the spread of the matrix entries, the dependence alone upon σ^2 , as well as a magnified/reduced gap do not imply any conclusion about the performance of the pertinent estimators.

Let us switch to the analysis of the bias. Table 1 shows how the biases pertaining to the different estimators depend upon the main problem parameters. All estimators depend upon the product Np_N (through the scaling sequence s_N), upon the constant κ , and upon the combination matrix spectral radius ρ . Notably, only the bias of the Granger estimator depends upon the fraction of monitored nodes ξ . This finding makes sense, since the Granger estimator is based upon inversion of a partial matrix (with the latent variables introducing error), whereas the one-lag and the residual estimator are natively determined only by pairwise interactions. In comparison, only the bias of the Granger estimator does not depend upon σ^2 , and this behavior is easily grasped in light of the explanation in the previous paragraph.

9. Illustrative Examples. It is useful to highlight the common structure adopted in the forthcoming examples. We consider the Granger, the one-lag, and the residual estimator, which are computed both under the assumption of unlimited sample sizes (*theoretical* correlation matrices, R_0 and R_1), as well as under the assumption of finite sample size (*empirical* correlation matrices). We compare the performance of the estimators in terms of the probability of correct graph recovery, evaluated through Monte Carlo simulations. The classification/thresholding stage are implemented through our modified k -means algorithm with $k = 2$, i.e., we do not rely on any a-priori knowledge of the system parameter to set the classification threshold. Finally, the input source samples, $\mathbf{x}_i(n)$, are i.i.d. samples from a standard Gaussian distribution, and we set $\sigma = 1$.

In Fig. 5, leftmost panel, we offer a sample of the behavior observed in the uniform-and-dense regime (constant connection probability). As a general comment, we see that all the estimators, both with unlimited or limited sample sizes, match well the theoretical predictions. In this particular

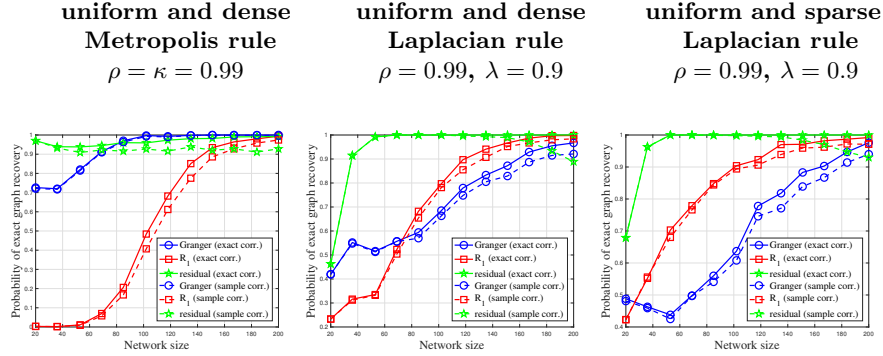


FIG 5. The figure displays the probability of correct graph recovery (estimated over 10^3 Monte Carlo runs) for the three estimators detailed in the legend, for both the cases where the correlation matrices are perfectly known, or where they are estimated from time samples. Each panel refers to a different setting, as explained in the title. The number of time samples used for the empirical correlation estimators is equal to 5×10^5 .

example, we observe that, after an initial transient with small network sizes, the Granger estimator outperforms the other two estimators. A legitimate question at this stage is whether or not this is a general behavior.

In order to answer, in the middle panel of Fig. 5 we consider a different setting, and we see that the residual estimator outperforms the one-lag estimator, which in turn outperforms the Granger estimator. *This is a remarkable finding*, since it highlights how the best estimator for the full-observability case (i.e., the Granger estimator) need not be optimal for a partial-observability setting. One reason behind the discrepancies between the leftmost and the middle panels has to be ascribed to the fact that, in the latter case, the fraction of observed nodes is reduced substantially. Perhaps unexpectedly, the Granger estimator is more sensitive to the degree of observability, whereas it tends to be more performing when one approaches the regime of full observability.

However, another remarkable finding is related to sample complexity since the middle panel in Fig. 5 highlights that the different estimators exhibit a different sensitivity to the number of samples adopted for the estimation. In particular, the residual estimator (which offers the best performance in the case of unlimited sample size) over finite amounts of data starts worsen around $N \approx 160$. Therefore, the other two estimators (Granger and one-lag) seems to be preferable for large network sizes (for a fixed size of the available time samples). It is difficult to quantify precisely these effects, since: *i*) the performance of the unlimited sample-size estimators is determined by the interplay between the gap and the inter-cluster variances, which is not easy

Estimator	Uniform concentration regime	Very sparse regime
Granger: $[\mathbf{R}_1]_s([\mathbf{R}_0]_s)^{-1}$	Universal local structural consistency	Mild consistency ⁴ [28]
one-lag: $[\mathbf{R}_1]_s$	Universal local structural consistency	?
residual: $[\mathbf{R}_1]_s - [\mathbf{R}_0]_s$	Universal local structural consistency	?

TABLE 2

Summary of the known and yet unknown consistency properties of the estimators considered in this work.

to evaluate analytically; *ii*) one must add the uncertainty related to the finite sample-size errors. It is the combined effect of these factors that ultimately determines the performance of a particular structure learning algorithm.

In order to complete the analysis, in the rightmost panel of Fig. 5 we show one example pertaining to the uniform-and-sparse regime, where we see that conclusions similar to those drawn for the uniform-and-dense regime apply.

10. Conclusion. This work examined the problem of graph learning when data can be collected from a limited subset of nodes. The goal is to learn the topology of the subgraph of monitored nodes. We considered one useful class of generative graph models, namely, the random graph Erdős-Rényi model. Three learning algorithms were developed, which were proved to be structurally consistent in the thermodynamic limit where the overall network size grows without bound. We explored various regimes of connectivity, including the often overlooked regime of *dense* connectivity. One revealing conclusion stemming from our analysis is that the *statistical concentration* of node degrees plays a central role for consistent graph learning, sometimes even more important than the *sparsity* of connections.

A succinct summary of the results is given in Table 2. This work focused on the uniform concentration regimes, whereas some results for the very sparse regime are already available from previous works. Moreover, we used question marks to highlight some open issues. We see that results about consistency under the very sparse regime (which was not dealt with here) are not available for the one-lag and for the residual estimators.

⁴Actually, for the Granger estimator under the very sparse regime, the available consistency result is a *mild consistency* result provided in terms of average fraction of errors.

There are further open issues that may deserve attention. One issue concerns *directed* graphs, which are relevant, e.g., in the context of causation. We believe that the graph-edge-domain approach developed in this work (more specifically, the recursive inequalities on the matrix-power entries provided in Appendix B) can be generalized to get insights about the directed graph setting.

This work focused on the Erdős-Rényi model, and used certain regularity assumptions on the diffusion matrix. A useful extension would be to examine structural consistency for other graph models, and/or under different regularity assumptions. For example, one might have a certain heterogeneity in the network (e.g., different connectivity across nodes), so as to observe multiple gaps in the estimated matrices, and an interesting question would be whether or not consistency can be achieved under these conditions.

Another open problem regards the search for *optimal* learning algorithms, where optimality can be formulated by taking into account the learning performance as well as the different sources of complexity. In this connection, complementing the analysis with a thorough characterization in terms of hardness and sample complexity would constitute a significant advance.

APPENDIX A: USEFUL PROPERTIES OF GRAPH DEGREES

We denote by $\mathcal{B}_i(N, q)$, with $i = 1, 2, \dots, K$, a sequence of K binomial random variables (not necessarily independent) with success probability q over N independent Bernoulli trials. Moreover, we denote by $\mathcal{B}_{\max}(N, q, K)$ and $\mathcal{B}_{\min}(N, q, K)$ the maximum and the minimum over this sequence, respectively. The following two relationships are standard inequalities arising from the application of the Chernoff bounding technique, and will be the fundamental building blocks to characterize the asymptotic behavior of several random quantities arising in our problem. The inequalities are as follows⁵.

⁵For any $t > 0$, we can write:

$$(A.1) \quad \mathbb{P}[\mathcal{B}_i(N, q) \geq x] = \mathbb{P}[e^{\mathcal{B}_i(N, q)t} \geq e^{xt}] \leq e^{-xt} \mathbb{E}[e^{\mathcal{B}_i(N, q)t}],$$

where the latter inequality is an application of Markov's inequality. Since a binomial variable of parameters N and q is the sum of N independent Bernoulli variables with success probability equal to q , we can further write:

$$(A.2) \quad \mathbb{E}[e^{\mathcal{B}_i(N, q)t}] = (qe^t + 1 - q)^N = (1 + q(e^t - 1))^N \leq e^{Nq(e^t - 1)},$$

where the latter inequality follows by observing that, for $z > 0$, one has $(1 + z)^N \leq e^{Nz}$. Combining (A.2) with (A.1) yields (A.3). Equation (A.4) is worked out with a similar technique.

For any $t > 0$:

$$(A.3) \quad \mathbb{P}[\mathcal{B}_{\max}(N, q, K) \geq x] \leq Ke^{-xt+Nq(e^t-1)},$$

$$(A.4) \quad \mathbb{P}[\mathcal{B}_{\min}(N, q, K) \leq x] \leq Ke^{xt-Nq(1-e^{-t})}.$$

We now apply these fundamental bounds to some specific random variables that are of interest in our setting.

We start by characterizing the behavior of the variables:

$$(A.5) \quad \mathcal{B}_{\max}(N, p_N, N), \quad \mathcal{B}_{\min}(N, p_N, N),$$

which, as we will see, are useful to characterize the behavior of the maximal and minimal degree of the graphs that we use in this work. The forthcoming lemma contains fundamental (classic) results about the asymptotic behavior of $\mathcal{B}_{\max}(N, p_N, N)$ and $\mathcal{B}_{\min}(N, p_N, N)$ under the different regimes for the probability p_N .

LEMMA 1 (Asymptotic scaling of $\mathcal{B}_{\max}(N, p_N, N)$ and $\mathcal{B}_{\min}(N, p_N, N)$).
 Let the probability p_N scale with N according to (5.5). Then:

$$(A.6) \quad \boxed{\frac{\mathcal{B}_{\max}(N, p_N, N)}{Np_N} \xrightarrow{p} 1, \quad \frac{\mathcal{B}_{\min}(N, p_N, N)}{Np_N} \xrightarrow{p} 1}$$

PROOF. The following inequality, holding for all $\epsilon > 0$, is easily obtained from (A.3) by setting $K = N$, $q = p_N$, $x = (1 + \epsilon)Np_N$, $t = \log(1 + \epsilon)$, and $g_\epsilon \triangleq 1 + [1 + \epsilon][\log(1 + \epsilon) - 1]$:

$$(A.7) \quad \mathbb{P}[\mathcal{B}_{\max}(N, p_N, N) \geq (1 + \epsilon)Np_N] \leq Ne^{-Np_Ng_\epsilon}.$$

Using now (5.5) in (A.8) we get:

$$(A.8) \quad \mathbb{P}[\mathcal{B}_{\max}(N, p_N, N) \geq (1 + \epsilon)Np_N] \leq N^{1-\omega_Ng_\epsilon} \xrightarrow{N \rightarrow \infty} 0,$$

which follows because $g_\epsilon > 0$ for all $\epsilon > 0$, as $g_0 = 0$ and $dg_\epsilon/d\epsilon > 0$ for all $\epsilon > 0$.

Likewise, the following inequality, holding for all $0 < \epsilon < 1$, is easily obtained from (A.4) by setting $K = N$, $q = p_N$, $x = (1 - \epsilon)Np_N$, $t = -\log(1 - \epsilon)$, and $h_\epsilon \triangleq 1 - [1 - \epsilon][1 - \log(1 - \epsilon)]$:

$$(A.9) \quad \mathbb{P}[\mathcal{B}_{\min}(N, p_N, N) \leq (1 - \epsilon)Np_N] \leq N^{1-\omega_Nh_\epsilon} \xrightarrow{N \rightarrow \infty} 0,$$

which follows because $h_\epsilon > 0$ for all $0 < \epsilon < 1$, as $h_0 = 0$ and $dh_\epsilon/d\epsilon > 0$ for all $0 < \epsilon < 1$. By joining (A.8) with (A.9), and observing that $\mathcal{B}_{\max}(N, p_N, N) \geq \mathcal{B}_{\min}(N, p_N, N)$, we conclude that (A.6) holds true. \square

As simple corollaries to Lemma 1, we can now obtain the characterization of the maximal and minimal degrees.

COROLLARY 1 (Behavior of \mathbf{d}_{\max} and \mathbf{d}_{\min}). *If the connection probability of the Erdős-Rényi model obeys (5.5), then we have:*

$$(A.10) \quad \boxed{\frac{\mathbf{d}_{\max}}{Np_N} \xrightarrow{P} 1, \quad \frac{\mathbf{d}_{\min}}{Np_N} \xrightarrow{P} 1, \quad [\text{Uniform concentration}]}$$

PROOF. The degree of a single node is equal to 1 plus (because in our setting the degree counts also the node itself) a binomial random variable with parameters $N - 1$ and p_N . Therefore, we have the following representation:

$$(A.11) \quad \mathbf{d}_{\max} = 1 + \mathcal{B}_{\max}(N - 1, p_N, N),$$

$$(A.12) \quad \mathbf{d}_{\min} = 1 + \mathcal{B}_{\min}(N - 1, p_N, N).$$

In order to obtain useful bounds involving \mathbf{d}_{\max} and \mathbf{d}_{\min} , let us introduce a modified sequence of binomial variables, obtained by adding one more Bernoulli trial to each binomial variable $\mathcal{B}_i(N, p_N)$, with $i = 1, 2, \dots, N$. The corresponding maximum and minimum taken over the modified sequence will be denoted by $\tilde{\mathcal{B}}_{\max}(N, p_N, N)$ and $\tilde{\mathcal{B}}_{\min}(N, p_N, N)$, respectively. Since a Bernoulli variable can be either zero or one, from (A.11) and (A.12) we get readily the following bounds:

$$(A.13) \quad \mathbf{d}_{\max} \leq 1 + \tilde{\mathcal{B}}_{\max}(N, p_N, N),$$

$$(A.14) \quad \mathbf{d}_{\min} \geq \tilde{\mathcal{B}}_{\min}(N, p_N, N),$$

and, hence, the claims of the corollary follow readily from Lemma 1, with the factor 1 playing no role as $N \rightarrow \infty$. \square

A.1. Another Useful Concentration Result.

LEMMA 2 (Maximum and minimum of N^2 binomial variables with success probability p_N^2). *Assume that the success probability obeys (5.5). Then we have that:*

$$(A.15) \quad \boxed{\frac{\mathcal{B}_{\max}(N, p_N^2, N^2)}{Np_N} \xrightarrow{P} p, \quad \frac{\mathcal{B}_{\min}(N, p_N^2, N^2)}{Np_N} \xrightarrow{P} p}$$

PROOF. If $p_N \rightarrow p > 0$, we can set $p'_N = p_N^2$, and obviously p'_N converges to $p^2 > 0$, implying that the binomial variables of parameters N and p'_N

are generated under the uniform concentration regime. The result in (A.15) then readily follows from (A.3) and (A.4).

If $p_N \rightarrow p = 0$, it suffices to prove the claim for the maximum. Applying (A.3) we can write:

$$(A.16) \quad \begin{aligned} \mathbb{P}[\mathcal{B}_{\max}(N, p_N^2, N^2) \geq \epsilon N p_N] &\leq N^2 e^{-N p_N [\epsilon t - p_N (e^t - 1)]} \\ &= N^2 N^{-\omega_N [\epsilon t - p_N (e^t - 1)]}. \end{aligned}$$

where, in the last step, we used the equality $N p_N = \omega_N \log N$ that follows from (5.5). Moreover, since we are considering the case where $p_N \rightarrow 0$ as $N \rightarrow \infty$, for any $\epsilon' > 0$ and for sufficiently large N we will have $p_N < \epsilon'$, so that, asymptotically, it is legitimate to replace (A.16) with:

$$(A.17) \quad \mathbb{P}[\mathcal{B}_{\max}(N, p_N^2, N^2) \geq \epsilon N p_N] \leq N^2 N^{-\omega_N [\epsilon t - \epsilon' (e^t - 1)]}.$$

Now, choosing ϵ' small enough so that $\epsilon' (e^t - 1) < \epsilon t$, we finally get:

$$(A.18) \quad \mathbb{P}[\mathcal{B}_{\max}(N, p_N^2, N^2) \geq \epsilon N p_N] \xrightarrow{N \rightarrow \infty} 0,$$

which completes the proof of the lemma. \square

APPENDIX B: USEFUL RECURSION ON MATRIX POWERS

The next two theorems establish some useful properties of the powers of matrix \mathbf{A} , and of the powers of matrix $\mathbf{C} \triangleq [\mathbf{A}^2]_{S'}$ that has been introduced in (7.4). In particular, the theorems will provide upper and lower bounds for the entries of the matrix powers in terms of two appropriately constructed stochastic processes. These upper and lower bounds will be useful to examine the concentration behavior of the estimators proposed in this work, namely, Theorem 3 will be useful for the Granger estimator, whereas Theorem 2 will be useful for the one-lag and for the residual estimators.

In the following, the symbol $\mathbf{a}_{ij}^{(k)}$ will denote the (i, j) -th entry of the k -th matrix power \mathbf{A}^k . Table 3 lists some useful random variables that are necessary to state and prove the theorems.

THEOREM 2 (Useful Recursion on the Powers of \mathbf{A}).

i) The entries of the combination matrix \mathbf{A} are bounded as follows:

$$(B.1) \quad \underline{\alpha}_k \leq \mathbf{a}_{ii}^{(k)} \leq \bar{\alpha}_k,$$

and, for $i \neq j$:

$$(B.2) \quad \underline{\beta}_k \mathbf{a}_{ij} + \underline{\gamma}_k \mathbf{m} \leq \mathbf{a}_{ij}^{(k)} \leq \bar{\beta}_k \mathbf{a}_{ij} + \bar{\gamma}_k \mathfrak{M},$$

where, for $k \geq 2$, the (random) sequences $\bar{\alpha}_k$, $\underline{\alpha}_k$, $\bar{\beta}_k$, $\underline{\beta}_k$, $\bar{\gamma}_k$, and $\underline{\gamma}_k$, are determined by the following recursions:

$$(B.3) \quad \begin{cases} \bar{\alpha}_{k+1} = \mathfrak{M}_{a,\text{self}} \bar{\alpha}_k + \mathfrak{M}_a \rho^k, \\ \bar{\beta}_{k+1} = \bar{\alpha}_k + \mathfrak{M}_{a,\text{self}} \bar{\beta}_k, \\ \bar{\gamma}_{k+1} = \bar{\beta}_k + \mathfrak{M}_{a,\text{sum}} \bar{\gamma}_k \end{cases}$$

with the initialization choices:

$$(B.4) \quad \bar{\alpha}_2 = \mathfrak{M}_{a_2,\text{self}}, \quad \bar{\beta}_2 = 2 \mathfrak{M}_{a,\text{self}}, \quad \bar{\gamma}_2 = 1,$$

and

$$(B.5) \quad \begin{cases} \underline{\alpha}_{k+1} = \mathfrak{m}_{a,\text{self}} \underline{\alpha}_k, \\ \underline{\beta}_{k+1} = \underline{\alpha}_k + \mathfrak{m}_{a,\text{self}} \underline{\beta}_k, \\ \underline{\gamma}_{k+1} = \underline{\beta}_k + \mathfrak{m}_{a,\text{sum}} \underline{\gamma}_k \end{cases}$$

with the initialization choices:

$$(B.6) \quad \underline{\alpha}_2 = \mathfrak{m}_{a_2,\text{self}}, \quad \underline{\beta}_2 = 2 \mathfrak{m}_{a,\text{self}}, \quad \underline{\gamma}_2 = 1.$$

ii) Let us introduce the following series:

$$(B.7) \quad \begin{aligned} \bar{\Sigma}_\alpha^{(\text{even})} &\triangleq \sum_{h=1}^{\infty} \bar{\alpha}_{2h}, & \underline{\Sigma}_\alpha^{(\text{even})} &\triangleq \sum_{h=1}^{\infty} \underline{\alpha}_{2h}, \\ \bar{\Sigma}_\beta^{(\text{even})} &\triangleq \sum_{h=1}^{\infty} \bar{\beta}_{2h}, & \underline{\Sigma}_\beta^{(\text{even})} &\triangleq \sum_{h=1}^{\infty} \underline{\beta}_{2h}, \\ \bar{\Sigma}_\gamma^{(\text{even})} &\triangleq \sum_{h=1}^{\infty} \bar{\gamma}_{2h}, & \underline{\Sigma}_\gamma^{(\text{even})} &\triangleq \sum_{h=1}^{\infty} \underline{\gamma}_{2h}, \end{aligned}$$

and

$$(B.8) \quad \begin{aligned} \bar{\Sigma}_\alpha^{(\text{odd})} &\triangleq \sum_{h=1}^{\infty} \bar{\alpha}_{2h+1}, & \underline{\Sigma}_\alpha^{(\text{odd})} &\triangleq \sum_{h=1}^{\infty} \underline{\alpha}_{2h+1}, \\ \bar{\Sigma}_\beta^{(\text{odd})} &\triangleq \sum_{h=1}^{\infty} \bar{\beta}_{2h+1}, & \underline{\Sigma}_\beta^{(\text{odd})} &\triangleq \sum_{h=1}^{\infty} \underline{\beta}_{2h+1}, \\ \bar{\Sigma}_\gamma^{(\text{odd})} &\triangleq \sum_{h=1}^{\infty} \bar{\gamma}_{2h+1}, & \underline{\Sigma}_\gamma^{(\text{odd})} &\triangleq \sum_{h=1}^{\infty} \underline{\gamma}_{2h+1}, \end{aligned}$$

with

$$\begin{aligned}
\bar{\Sigma}_\alpha &\triangleq \bar{\Sigma}_\alpha^{(\text{even})} + \bar{\Sigma}_\alpha^{(\text{odd})}, & \underline{\Sigma}_\alpha &\triangleq \underline{\Sigma}_\alpha^{(\text{even})} + \underline{\Sigma}_\alpha^{(\text{odd})}, \\
\bar{\Sigma}_\beta &\triangleq \bar{\Sigma}_\beta^{(\text{even})} + \bar{\Sigma}_\beta^{(\text{odd})}, & \underline{\Sigma}_\beta &\triangleq \underline{\Sigma}_\beta^{(\text{even})} + \underline{\Sigma}_\beta^{(\text{odd})}, \\
\bar{\Sigma}_\gamma &\triangleq \bar{\Sigma}_\gamma^{(\text{even})} + \bar{\Sigma}_\gamma^{(\text{odd})}, & \underline{\Sigma}_\gamma &\triangleq \underline{\Sigma}_\gamma^{(\text{even})} + \underline{\Sigma}_\gamma^{(\text{odd})}.
\end{aligned}
\tag{B.9}$$

Let $\zeta = \rho - \kappa$. Under the uniform concentration regime, the following convergences in probability hold.

$$\begin{aligned}
\bar{\Sigma}_\alpha \text{ and } \underline{\Sigma}_\alpha &\xrightarrow{\text{p}} \frac{\zeta^2}{1 - \zeta}, \\
\bar{\Sigma}_\beta \text{ and } \underline{\Sigma}_\beta &\xrightarrow{\text{p}} \frac{1 - (1 - \zeta)^2}{(1 - \zeta)^2}, \\
\bar{\Sigma}_\gamma \text{ and } \underline{\Sigma}_\gamma &\xrightarrow{\text{p}} \frac{1}{(1 - \rho)(1 - \zeta)^2}
\end{aligned}
\tag{B.10}$$

$$\begin{aligned}
\bar{\Sigma}_\alpha^{(\text{even})} \text{ and } \underline{\Sigma}_\alpha^{(\text{even})} &\xrightarrow{\text{p}} \frac{\zeta^2}{1 - \zeta^2}, \\
\bar{\Sigma}_\beta^{(\text{even})} \text{ and } \underline{\Sigma}_\beta^{(\text{even})} &\xrightarrow{\text{p}} \frac{2\zeta}{(1 - \zeta^2)^2}, \\
\bar{\Sigma}_\gamma^{(\text{even})} \text{ and } \underline{\Sigma}_\gamma^{(\text{even})} &\xrightarrow{\text{p}} \frac{1 + \zeta^2 + 2\rho\zeta}{(1 - \rho)(1 - \zeta^2)^2},
\end{aligned}
\tag{B.11}$$

$$\begin{aligned}
\bar{\Sigma}_\alpha^{(\text{odd})} \text{ and } \underline{\Sigma}_\alpha^{(\text{odd})} &\xrightarrow{\text{p}} \frac{\zeta^3}{1 - \zeta^2}, \\
\bar{\Sigma}_\beta^{(\text{odd})} \text{ and } \underline{\Sigma}_\beta^{(\text{odd})} &\xrightarrow{\text{p}} \frac{3\zeta^2 - \zeta^4}{(1 - \zeta^2)^2}, \\
\bar{\Sigma}_\gamma^{(\text{odd})} \text{ and } \underline{\Sigma}_\gamma^{(\text{odd})} &\xrightarrow{\text{p}} \frac{\rho + \rho\zeta^2 + 2\zeta}{(1 - \rho)(1 - \zeta^2)^2},
\end{aligned}
\tag{B.12}$$

PROOF. We start by examining the relationships pertaining to the main diagonal terms, namely, Eq. (B.1). For $k = 2$ the claim is trivially true with the values of $\bar{\alpha}_2$ and $\underline{\alpha}_2$ in (B.4) and (B.6), because of the definitions 3) and 4) in Table 3. We shall therefore reason by induction to prove that (B.1) holds for an arbitrary k . In particular, we assume the claim verified for k ,

and manage to prove that it is verified for $k + 1$. To this aim, we start by writing the diagonal terms of the $(k + 1)$ -th matrix power as:

$$(B.13) \quad \mathbf{a}_{ii}^{(k+1)} = \sum_{\ell \in \mathcal{N}} \mathbf{a}_{i\ell} \mathbf{a}_{\ell i}^{(k)} = \mathbf{a}_{ii} \mathbf{a}_{ii}^{(k)} + \sum_{\substack{\ell \in \mathcal{N} \\ \ell \neq i}} \mathbf{a}_{i\ell} \mathbf{a}_{\ell i}^{(k)},$$

and, hence:

$$(B.14) \quad \mathbf{a}_{ii} \mathbf{a}_{ii}^{(k)} \leq \mathbf{a}_{ii}^{(k+1)} \leq \mathbf{a}_{ii} \mathbf{a}_{ii}^{(k)} + \mathfrak{M}_a \rho^k,$$

where we have used the fact that $\sum_{\ell \in \mathcal{N}} \mathbf{a}_{\ell i}^{(k)} = \rho^k$ along with definition 1) in Table 3. Since we have assumed that (B.1) is true for k , from (B.14) we also have:

$$(B.15) \quad \mathbf{m}_{a,\text{self}} \underline{\alpha}_k \leq \mathbf{a}_{ii}^{(k+1)} \leq \mathfrak{M}_{a,\text{self}} \bar{\alpha}_k + \mathfrak{M}_a \rho^k,$$

from which we conclude that (B.1) holds true, with the sequences $\bar{\alpha}_k$ and $\underline{\alpha}_k$ obeying the recursions in (B.3) and (B.5), respectively.

We switch to the proof of (B.2). First, we observe that (B.43) implies that (B.2) holds true in the case $k = 2$, with the choices detailed in (B.35) and (B.37). Moreover, we have:

$$(B.16) \quad \mathbf{a}_{ij}^{(k+1)} = \sum_{\ell \in \mathcal{N}} \mathbf{a}_{i\ell} \mathbf{a}_{\ell j}^{(k)} = \mathbf{a}_{ij} \mathbf{a}_{jj}^{(k)} + \sum_{\substack{\ell \in \mathcal{N} \\ \ell \neq j}} \mathbf{a}_{i\ell} \mathbf{a}_{\ell j}^{(k)}.$$

Therefore, since (B.1) holds true, and assuming that (B.2) holds for an arbitrary $k \geq 2$, we have:

$$(B.17) \quad \begin{aligned} \mathbf{a}_{ij}^{(k+1)} &\leq \bar{\alpha}_k \mathbf{a}_{ij} + \bar{\beta}_k \sum_{\substack{\ell \in \mathcal{N} \\ \ell \neq j}} \mathbf{a}_{i\ell} \mathbf{a}_{\ell j} + \bar{\gamma}_k \mathfrak{M} \sum_{\substack{\ell \in \mathcal{N} \\ \ell \neq j}} \mathbf{a}_{\ell j} \\ &\leq (\bar{\alpha}_k + \bar{\beta}_k \mathfrak{M}_{a,\text{self}}) \mathbf{a}_{ij} + (\bar{\beta}_k + \bar{\gamma}_k \mathfrak{M}_{a,\text{sum}}) \mathfrak{M}, \end{aligned}$$

which shows that the rightmost inequality in (B.2) holds with the sequences $\bar{\beta}_k$ and $\bar{\gamma}_k$ obeying (B.3), and with the initialization choice in (B.4).

Next we focus on proving part ii). First, we notice that all the involved series are convergent. We will explain this conclusion with reference to the upper bounding sequences, with the case of the lower bounding sequences being dealt with similarly. The system of recursions in (B.3) can be solved by calculating first $\bar{\alpha}_k$, then $\bar{\beta}_k$ (after substituting $\bar{\alpha}_k$) and finally $\bar{\gamma}_k$ (after

substituting $\bar{\beta}_k$). Applying Lemma 5, it can be verified that all the obtained solutions are linear combinations of geometric sequences with ratio strictly smaller than one, from which convergence of the series $\bar{\Sigma}_\alpha$, $\bar{\Sigma}_\beta$ and $\bar{\Sigma}_\gamma$ follows.

First of all, it is convenient to rewrite the series in (B.9) in the following more explicit form:

$$(B.18) \quad \begin{aligned} \bar{\Sigma}_\alpha &\triangleq \sum_{k=2}^{\infty} \bar{\alpha}_k, & \underline{\Sigma}_\alpha &\triangleq \sum_{k=2}^{\infty} \underline{\alpha}_k, \\ \bar{\Sigma}_\beta &\triangleq \sum_{k=2}^{\infty} \bar{\beta}_k, & \underline{\Sigma}_\beta &\triangleq \sum_{k=2}^{\infty} \underline{\beta}_k, \\ \bar{\Sigma}_\gamma &\triangleq \sum_{k=2}^{\infty} \bar{\gamma}_k, & \underline{\Sigma}_\gamma &\triangleq \sum_{k=2}^{\infty} \underline{\gamma}_k. \end{aligned}$$

Let us consider the first line in (B.3). By summing over index k , and using the definition of $\bar{\Sigma}_\alpha$ in (B.18), we can write:

$$(B.19) \quad \bar{\Sigma}_\alpha = \bar{\alpha}_2 + \mathfrak{M}_{a,\text{self}} \bar{\Sigma}_\alpha + \frac{\mathfrak{M}_a \rho^2}{1 - \rho} \Rightarrow \bar{\Sigma}_\alpha = \frac{\mathfrak{M}_{a2,\text{self}} + \epsilon}{1 - \mathfrak{M}_{a,\text{self}}}.$$

where we have set $\epsilon = \frac{\mathfrak{M}_a \rho^2}{1 - \rho}$. Likewise, operating on the second line in (B.3), and using the definition of $\bar{\Sigma}_\beta$ in (B.18), we get:

$$(B.20) \quad \bar{\Sigma}_\beta = \bar{\beta}_2 + \bar{\Sigma}_\alpha + \mathfrak{M}_{a,\text{self}} \bar{\Sigma}_\beta \Rightarrow \bar{\Sigma}_\beta = \frac{2 \mathfrak{M}_{a,\text{self}} + \bar{\Sigma}_\alpha}{1 - \mathfrak{M}_{a,\text{self}}}.$$

Finally, repeating the above procedure over the third line of (B.3), we obtain:

$$(B.21) \quad \bar{\Sigma}_\gamma = \bar{\gamma}_2 + \bar{\Sigma}_\beta + \mathfrak{M}_{a,\text{sum}} \bar{\Sigma}_\gamma \Rightarrow \bar{\Sigma}_\gamma = \frac{1 + \bar{\Sigma}_\beta}{1 - \mathfrak{M}_{a,\text{sum}}},$$

which, using (B.19) and (B.20), after straightforward algebra yields:

$$(B.22) \quad \bar{\Sigma}_\gamma = \frac{1 - \mathfrak{M}_{a,\text{self}}^2 + \mathfrak{M}_{a2,\text{self}} + \epsilon}{(1 - \mathfrak{M}_{a,\text{sum}})(1 - \mathfrak{M}_{a,\text{self}})^2}.$$

Now, in view of the convergences in probability proved in Lemma 4 — specifically, in view of (D.1), (D.4), (D.7) — it is legitimate to replace the pertinent variables in (B.19), (B.20), and (B.22), with their limits (that are reported in Table 3). After some lengthy, though straightforward, algebra, this replacement leads to (B.10).

We now move on to prove (B.12). Using the definitions of $\overline{\Sigma}_\alpha^{(\text{even})}$ and $\overline{\Sigma}_\alpha^{(\text{odd})}$ in (B.7) and (B.8), and summing over k the first line in (B.3), we see that:

$$\begin{aligned}
\overline{\Sigma}_\alpha^{(\text{odd})} &= \sum_{\substack{k=3 \\ k \text{ odd}}}^{\infty} \overline{\alpha}_k = \sum_{\substack{k=2 \\ k \text{ even}}}^{\infty} \overline{\alpha}_{k+1} \\
&= \mathfrak{M}_{a,\text{self}} \sum_{\substack{k=2 \\ k \text{ even}}}^{\infty} \overline{\alpha}_k + \mathfrak{M}_a \sum_{\substack{k=2 \\ k \text{ even}}}^{\infty} \rho^k \\
&= \mathfrak{M}_{a,\text{self}} \overline{\Sigma}_\alpha^{(\text{even})} + \mathfrak{M}_a \sum_{k=1}^{\infty} \rho^{2k} \\
&= \mathfrak{M}_{a,\text{self}} \overline{\Sigma}_\alpha - \mathfrak{M}_{a,\text{self}} \overline{\Sigma}_\alpha^{(\text{odd})} + \mathfrak{M}_a \frac{\rho^2}{1 - \rho^2},
\end{aligned}
\tag{B.23}$$

yielding:

$$\overline{\Sigma}_\alpha^{(\text{odd})} = \frac{\mathfrak{M}_{a,\text{self}} \overline{\Sigma}_\alpha + \epsilon'}{1 + \mathfrak{M}_{a,\text{self}}}
\tag{B.24}$$

where we defined $\epsilon' = \mathfrak{M}_a \frac{\rho^2}{1 - \rho^2}$. Using now (B.9) and (B.24), we further obtain:

$$\overline{\Sigma}_\alpha^{(\text{even})} = \frac{\overline{\Sigma}_\alpha - \epsilon'}{1 + \mathfrak{M}_{a,\text{self}}}
\tag{B.25}$$

Proceeding in a similar way, from the second relationship in (B.3), we obtain:

$$\begin{aligned}
\overline{\Sigma}_\beta^{(\text{odd})} &= \overline{\Sigma}_\alpha^{(\text{even})} + \mathfrak{M}_{a,\text{self}} \overline{\Sigma}_\beta^{(\text{even})} \\
&= \overline{\Sigma}_\alpha^{(\text{even})} + \mathfrak{M}_{a,\text{self}} \overline{\Sigma}_\beta - \mathfrak{M}_{a,\text{self}} \overline{\Sigma}_\beta^{(\text{odd})},
\end{aligned}
\tag{B.26}$$

yielding:

$$\overline{\Sigma}_\beta^{(\text{odd})} = \frac{\mathfrak{M}_{a,\text{self}} \overline{\Sigma}_\beta + \overline{\Sigma}_\alpha^{(\text{even})}}{1 + \mathfrak{M}_{a,\text{self}}}
\tag{B.27}$$

and

$$\overline{\Sigma}_\beta^{(\text{even})} = \frac{\overline{\Sigma}_\beta - \overline{\Sigma}_\alpha^{(\text{even})}}{1 + \mathfrak{M}_{a,\text{self}}}
\tag{B.28}$$

Finally, from the third relationship in (B.3), we can write:

$$\begin{aligned}
 \overline{\Sigma}_\gamma^{(\text{odd})} &= \overline{\Sigma}_\beta^{(\text{even})} + \mathfrak{M}_{a,\text{sum}} \overline{\Sigma}_\gamma^{(\text{even})} \\
 \text{(B.29)} \quad &= \overline{\Sigma}_\beta^{(\text{even})} + \mathfrak{M}_{a,\text{sum}} \overline{\Sigma}_\gamma - \mathfrak{M}_{a,\text{sum}} \overline{\Sigma}_\beta^{(\text{odd})},
 \end{aligned}$$

yielding:

$$\text{(B.30)} \quad \boxed{\overline{\Sigma}_\gamma^{(\text{odd})} = \frac{\mathfrak{M}_{a,\text{sum}} \overline{\Sigma}_\gamma + \overline{\Sigma}_\beta^{(\text{even})}}{1 + \mathfrak{M}_{a,\text{sum}}}}$$

and

$$\text{(B.31)} \quad \boxed{\overline{\Sigma}_\gamma^{(\text{even})} = \frac{\overline{\Sigma}_\gamma - \overline{\Sigma}_\beta^{(\text{even})}}{1 + \mathfrak{M}_{a,\text{sum}}}}$$

The limiting results in (B.11) and (B.12) are now obtained by replacing, in (B.24), (B.25), (B.27), (B.28), (B.30), and (B.31), the pertinent random variables with their limiting counterparts shown in Table 3. \square

THEOREM 3 (Recursion Useful for the Granger Estimator).

i) The entries of the matrix \mathbf{C}^k are bounded as follows:

$$\text{(B.32)} \quad \underline{\alpha}_k \leq \mathbf{c}_{\ell\ell}^{(k)} \leq \overline{\alpha}_k,$$

and, for $\ell \neq m$:

$$\text{(B.33)} \quad \underline{\beta}_k \mathbf{a}_{\ell m} + \underline{\gamma}_k \leq \mathbf{c}_{\ell m}^{(k)} \leq \overline{\beta}_k \mathbf{a}_{\ell m} + \overline{\gamma}_k,$$

where, for $k \geq 1$, the (random) sequences $\overline{\alpha}_k$, $\underline{\alpha}_k$, $\overline{\beta}_k$, $\underline{\beta}_k$, $\overline{\gamma}_k$, and $\underline{\gamma}_k$, are determined by the following recursions:

$$\text{(B.34)} \quad \boxed{
 \begin{aligned}
 \overline{\alpha}_{k+1} &= \mathfrak{M}_{c,\text{self}} \overline{\alpha}_k + (2 \mathfrak{M}_{a,\text{self}} \mathfrak{M}_a + \mathfrak{M}) \rho^{2k}, \\
 \overline{\beta}_{k+1} &= 2 \mathfrak{M}_{a,\text{self}} \overline{\alpha}_k + \mathfrak{M}_{c,\text{self}} \overline{\beta}_k, \\
 \overline{\gamma}_{k+1} &= \mathfrak{M} \overline{\alpha}_k + (2 \mathfrak{M}_{a,\text{self}} \mathfrak{M}^{(s')} + \mathfrak{M} \mathfrak{M}_{a,\text{sum}}^{(s')}) \overline{\beta}_k \\
 &\quad + \mathfrak{M}_{c,\text{sum}} \overline{\gamma}_k
 \end{aligned}
 }$$

with the initialization choices:

$$\text{(B.35)} \quad \overline{\alpha}_1 = \mathfrak{M}_{c,\text{self}}, \quad \overline{\beta}_1 = 2 \mathfrak{M}_{a,\text{self}}, \quad \overline{\gamma}_1 = \mathfrak{M},$$

and

$$\begin{aligned}
 \underline{\alpha}_{k+1} &= \mathbf{m}_{c,\text{self}} \underline{\alpha}_k, \\
 \underline{\beta}_{k+1} &= 2 \mathbf{m}_{a,\text{self}} \underline{\alpha}_k + \mathbf{m}_{c,\text{self}} \underline{\beta}_k, \\
 \underline{\gamma}_{k+1} &= \mathbf{m} \underline{\alpha}_k + (2 \mathbf{m}_{a,\text{self}} \mathbf{m}^{(S')} + \mathbf{m} \mathbf{m}_{a,\text{sum}}^{(S')}) \underline{\beta}_k \\
 &\quad + \mathbf{m}_{c,\text{sum}} \underline{\gamma}_k
 \end{aligned}
 \tag{B.36}$$

with the initialization choices:

$$\underline{\alpha}_1 = \mathbf{m}_{c,\text{self}}, \quad \underline{\beta}_1 = 2 \mathbf{m}_{a,\text{self}}, \quad \underline{\gamma}_1 = \mathbf{m}.
 \tag{B.37}$$

ii) Let us introduce the following series:

$$\begin{aligned}
 \overline{\Sigma}_\alpha &\triangleq \sum_{k=1}^{\infty} \overline{\alpha}_k, & \underline{\Sigma}_\alpha &\triangleq \sum_{k=1}^{\infty} \underline{\alpha}_k, \\
 \overline{\Sigma}_\beta &\triangleq \sum_{k=1}^{\infty} \overline{\beta}_k, & \underline{\Sigma}_\beta &\triangleq \sum_{k=1}^{\infty} \underline{\beta}_k, \\
 \overline{\Sigma}_\gamma &\triangleq \sum_{k=1}^{\infty} \overline{\gamma}_k, & \underline{\Sigma}_\gamma &\triangleq \sum_{k=1}^{\infty} \underline{\gamma}_k.
 \end{aligned}
 \tag{B.38}$$

The entries of the matrix \mathbf{H} in (7.4) are bounded as follows:

$$1 + \underline{\Sigma}_\alpha \leq \mathbf{h}_{\ell\ell} \leq 1 + \overline{\Sigma}_\alpha,
 \tag{B.39}$$

and, for $\ell \neq m$:

$$\underline{\Sigma}_\beta \mathbf{a}_{\ell m} + \underline{\Sigma}_\gamma \leq \mathbf{h}_{\ell m} \leq \overline{\Sigma}_\beta \mathbf{a}_{\ell m} + \overline{\Sigma}_\gamma.
 \tag{B.40}$$

iii) Let $\zeta = \rho - \kappa$. Under the uniform concentration regime, we have the following convergences in probability:

$$\begin{aligned}
 \overline{\Sigma}_\alpha \text{ and } \underline{\Sigma}_\alpha &\xrightarrow{\text{P}} \frac{\zeta^2}{1 - \zeta^2}, \\
 \overline{\Sigma}_\beta \text{ and } \underline{\Sigma}_\beta &\xrightarrow{\text{P}} \frac{2\zeta}{(1 - \zeta^2)^2}, \\
 N p_N \overline{\Sigma}_\gamma \text{ and } N p_N \underline{\Sigma}_\gamma &\xrightarrow{\text{P}} \eta
 \end{aligned}
 \tag{B.41}$$

where

$$(B.42) \quad \eta \triangleq \kappa^2 p \frac{1 - \zeta^2 + 2\zeta[2\zeta(1 - \xi) + \kappa(1 - \xi)]}{[1 - (\rho^2 - 2\rho\kappa\xi + \kappa^2\xi)][1 - \zeta^2]^2}.$$

PROOF. We start with the inequalities pertaining to the main diagonal of matrices \mathbf{C}^k , namely, with (B.32). For $k = 1$ we use the definitions of $\bar{\alpha}_1$ and $\underline{\alpha}_1$ in (B.35) and (B.37), respectively, to see that (B.32) is trivially satisfied in view of definition 5) in Table 3. We shall now prove that (B.32) holds for an arbitrary k by induction. Assume thus that (B.32) is true for k , we need to show that it is true for $k + 1$. To this end, we observe preliminarily that, for all $i, j \in \mathcal{N}$, with $i \neq j$, we have:

$$(B.43) \quad \begin{aligned} \mathbf{a}_{ij}^{(2)} &= \sum_{\ell \in \mathcal{N}} \mathbf{a}_{i\ell} \mathbf{a}_{\ell j} = (\mathbf{a}_{ii} + \mathbf{a}_{jj}) \mathbf{a}_{ij} + \sum_{\substack{\ell \in \mathcal{N} \\ \ell \neq i, j}} \mathbf{a}_{i\ell} \mathbf{a}_{\ell j} \\ &\leq 2\mathfrak{M}_{a, \text{self}} \mathbf{a}_{ij} + \mathfrak{M} \leq 2\mathfrak{M}_{a, \text{self}} \mathfrak{M}_a + \mathfrak{M}, \end{aligned}$$

where we have applied the definitions 1), 2) and 12) in Table 3. On the other hand, from the definition of matrix \mathbf{C} in (7.4), we can write its terms on the main diagonal as:

$$(B.44) \quad \mathbf{c}_{\ell\ell}^{(k+1)} = \sum_{h \in \mathcal{S}'} \mathbf{c}_{\ell h} \mathbf{c}_{h\ell}^{(k)} = \mathbf{c}_{\ell\ell} \mathbf{c}_{\ell\ell}^{(k)} + \sum_{\substack{h \in \mathcal{S}' \\ h \neq \ell}} \mathbf{c}_{\ell h} \mathbf{c}_{h\ell}^{(k)}.$$

In view of (B.43) we can write:

$$(B.45) \quad \sum_{\substack{h \in \mathcal{S}' \\ h \neq \ell}} \mathbf{c}_{\ell h} \mathbf{c}_{h\ell}^{(k)} = \sum_{\substack{h \in \mathcal{S}' \\ h \neq \ell}} \mathbf{a}_{\ell h}^{(2)} \mathbf{c}_{h\ell}^{(k)} \leq (2\mathfrak{M}_{a, \text{self}} \mathfrak{M}_a + \mathfrak{M}) \sum_{\substack{h \in \mathcal{S}' \\ h \neq \ell}} \mathbf{c}_{h\ell}^{(k)}.$$

Moreover, we observe that:

$$(B.46) \quad \sum_{\substack{h \in \mathcal{S}' \\ h \neq \ell}} \mathbf{c}_{h\ell} \leq \sum_{h \in \mathcal{N}} \mathbf{c}_{h\ell} = \sum_{h \in \mathcal{N}} \mathbf{a}_{h\ell}^{(2)} = \rho^{2k},$$

where the last equality follows from the first relationship in (5.8) and from the symmetry of matrix \mathbf{A} . Therefore, we conclude that:

$$(B.47) \quad \mathfrak{m}_{c, \text{self}} \mathbf{c}_{\ell\ell}^{(k)} \leq \mathbf{c}_{\ell\ell}^{(k+1)} \leq \mathfrak{M}_{c, \text{self}} \mathbf{c}_{\ell\ell}^{(k)} + (2\mathfrak{M}_{a, \text{self}} \mathfrak{M}_a + \mathfrak{M}) \rho^{2k},$$

Since we have assumed that (B.32) holds true for k , we can further apply (B.32) into (B.47), yielding:

$$(B.48) \quad \mathfrak{m}_{c, \text{self}} \underline{\alpha}_k \leq \mathbf{c}_{\ell\ell}^{(k+1)} \leq \mathfrak{M}_{c, \text{self}} \bar{\alpha}_k + (2\mathfrak{M}_{a, \text{self}} \mathfrak{M}_a + \mathfrak{M}) \rho^{2k},$$

which reveals that (B.32) holds true, with the sequences $\bar{\alpha}_k$ and $\underline{\alpha}_k$ obeying the recursions in (B.34) and (B.36), respectively.

Let us move on to examine the case $\ell \neq m$. For all $\ell, m \in S'$, with $\ell \neq m$, we can use (B.43) to conclude that:

$$(B.49) \quad \mathbf{c}_{\ell m} \leq 2 \mathfrak{M}_{a, \text{self}} \mathbf{a}_{\ell m} + \mathfrak{M}.$$

Equation (B.49) shows that the upper bound in (B.33) holds for $k = 1$, with the choices in (B.35). Now, rewriting the relationship $\mathbf{C}^{k+1} = \mathbf{C}\mathbf{C}^k$ on an entrywise basis, we have:

$$(B.50) \quad \begin{aligned} \mathbf{c}_{\ell m}^{(k+1)} &= \sum_{h \in S'} \mathbf{c}_{\ell h} \mathbf{c}_{hm}^{(k)} \\ &= \mathbf{c}_{\ell m} \mathbf{c}_{mm}^{(k)} + \sum_{\substack{h \in S' \\ h \neq m}} \mathbf{c}_{\ell h} \mathbf{c}_{hm}^{(k)}. \end{aligned}$$

Accordingly, if we assume that (B.33) holds true for an arbitrary k , from (B.50) we get:

$$(B.51) \quad \begin{aligned} \mathbf{c}_{\ell m}^{(k+1)} &\leq \bar{\alpha}_k (2 \mathfrak{M}_{a, \text{self}} \mathbf{a}_{\ell m} + \mathfrak{M}) \\ &+ \bar{\beta}_k \sum_{\substack{h \in S' \\ h \neq m}} \mathbf{c}_{\ell h} \mathbf{a}_{hm} + \bar{\gamma}_k \sum_{\substack{h \in S' \\ h \neq m}} \mathbf{c}_{\ell h}. \end{aligned}$$

Focusing on the first summation, using definition 5) in Table 3 to bound the term \mathbf{c}_{ℓ} , and (B.49) to bound the term $\mathbf{c}_{\ell h}$, we get:

$$(B.52) \quad \begin{aligned} \sum_{\substack{h \in S' \\ h \neq m}} \mathbf{c}_{\ell h} \mathbf{a}_{hm} &= \mathbf{c}_{\ell \ell} \mathbf{a}_{\ell m} + \sum_{\substack{h \in S' \\ h \neq \ell, m}} \mathbf{c}_{\ell h} \mathbf{a}_{hm} \\ &\leq \mathfrak{M}_{c, \text{self}} \mathbf{a}_{\ell m} + 2 \mathfrak{M}_{a, \text{self}} \sum_{\substack{h \in S' \\ h \neq \ell, m}} \mathbf{a}_{\ell h} \mathbf{a}_{hm} \\ &+ \mathfrak{M} \sum_{\substack{h \in S' \\ h \neq \ell, m}} \mathbf{a}_{hm} \\ &\leq \mathfrak{M}_{c, \text{self}} \mathbf{a}_{\ell m} + 2 \mathfrak{M}_{a, \text{self}} \mathfrak{M}^{(S')} + \mathfrak{M} \mathfrak{M}_{a, \text{sum}}^{(S')}, \end{aligned}$$

where, in the latter inequality, we have further applied the definitions 7) and

13) in Table 3. Using now (B.52) into (B.51), we get:

$$\begin{aligned}
 \mathbf{c}_{\ell m}^{(k+1)} &\leq \underbrace{(2\mathfrak{M}_{a,\text{self}}\bar{\alpha}_k + \mathfrak{M}_{c,\text{self}}\bar{\beta}_k)}_{\bar{\beta}_{k+1}} \mathbf{a}_{\ell m} \\
 &+ \underbrace{[\mathfrak{M}\bar{\alpha}_k + (2\mathfrak{M}_{a,\text{self}}\mathfrak{M}^{(S')} + \mathfrak{M}\mathfrak{M}_{a,\text{sum}}^{(S')})\bar{\beta}_k + \mathfrak{M}_{c,\text{sum}}\bar{\gamma}_k]}_{\bar{\gamma}_{k+1}},
 \end{aligned}
 \tag{B.53}$$

which shows that (B.33) holds also for $k+1$, with $\bar{\beta}_k$, and $\bar{\gamma}_k$ obeying the recursion in (B.34). The proof of (B.36) is similar. This concludes part i) of the theorem. Part ii) comes readily as a corollary of part i), after noticing that the matrix \mathbf{H} defined in (7.4) can be expressed as $\mathbf{H} = (I_{N-K} - \mathbf{C})^{-1} = I_{N-K} + \mathbf{C} + \mathbf{C}^2 + \dots$, and summing the inequalities in (B.32) and (B.33) over index k . Convergence of all the involved series is guaranteed by Lemma 5.

Next we focus on proving part iii). Preliminarily, we observe that all the involved series are convergent. We will explain this conclusion with reference to the upper bounding sequences, with the case of the lower bounding sequences being dealt with similarly. The system of recursions in (B.34) can be solved by calculating first $\bar{\alpha}_k$, then $\bar{\beta}_k$ (after substituting $\bar{\alpha}_k$) and finally $\bar{\gamma}_k$ (after substituting $\bar{\beta}_k$). Applying Lemma 5, it can be verified that all the obtained solutions are linear combinations of geometric sequences with ratio strictly smaller than one, from which convergence of the series $\bar{\Sigma}_\alpha$, $\bar{\Sigma}_\beta$ and $\bar{\Sigma}_\gamma$ follows.

Let us consider the first line in (B.34). By summing over index k , and recalling the definition of $\bar{\Sigma}_\alpha$ in (B.38), we can write:

$$\bar{\Sigma}_\alpha = \bar{\alpha}_1 + \mathfrak{M}_{c,\text{self}}\bar{\Sigma}_\alpha + \epsilon \Rightarrow \bar{\Sigma}_\alpha = \frac{\mathfrak{M}_{c,\text{self}} + \epsilon}{1 - \mathfrak{M}_{c,\text{self}}},
 \tag{B.54}$$

where we have set

$$\epsilon = (2\mathfrak{M}_{a,\text{self}}\mathfrak{M}_a + \mathfrak{M}) \frac{\rho^2}{1 - \rho^2}.
 \tag{B.55}$$

Likewise, from the second line in (B.34), summing over index k , and recalling the definition of $\bar{\Sigma}_\beta$ in (B.38), we can write:

$$\bar{\Sigma}_\beta = \bar{\beta}_1 + 2\mathfrak{M}_{a,\text{self}}\bar{\Sigma}_\alpha + \mathfrak{M}_{c,\text{self}}\bar{\Sigma}_\beta,
 \tag{B.56}$$

yielding:

$$\bar{\Sigma}_\beta = \frac{2\mathfrak{M}_{a,\text{self}}(1 + \bar{\Sigma}_\alpha)}{1 - \mathfrak{M}_{c,\text{self}}}.
 \tag{B.57}$$

Using now (B.54) into (B.57), we get:

$$(B.58) \quad \bar{\Sigma}_\beta = \frac{2 \mathfrak{M}_{a,\text{self}}}{(1 - \mathfrak{M}_{c,\text{self}})^2} (1 + \epsilon).$$

Finally, repeating the same procedure on the third line in (B.34), we obtain:

$$(B.59) \quad \begin{aligned} \bar{\Sigma}_\gamma &= \bar{\gamma}_1 + \mathfrak{M} \bar{\Sigma}_\alpha + (2 \mathfrak{M}_{a,\text{self}} \mathfrak{M}^{(s')} + \mathfrak{M} \mathfrak{M}_{a,\text{sum}}^{(s')}) \bar{\Sigma}_\beta \\ &+ \mathfrak{M}_{c,\text{sum}} \bar{\Sigma}_\gamma, \end{aligned}$$

which yields the solution:

$$(B.60) \quad \bar{\Sigma}_\gamma = \frac{\mathfrak{M}(1 + \bar{\Sigma}_\alpha) + (2 \mathfrak{M}_{a,\text{self}} \mathfrak{M}^{(s')} + \mathfrak{M} \mathfrak{M}_{a,\text{sum}}^{(s')}) \bar{\Sigma}_\beta}{1 - \mathfrak{M}_{c,\text{sum}}}.$$

Now, in view of the convergences in probability proved in Lemma 4 — specifically, in view of (D.1), (D.10), (D.19), (D.20) and (D.26) — it is legitimate to replace the pertinent variables with their limits (that are reported in Table 3) in (B.54), (B.57), and (B.60), which, after some lengthy, though straightforward, algebra, leads to (B.41). \square

APPENDIX C: PROOF OF THEOREM ??

We start by proving an auxiliary lemma.

LEMMA 3 (Sufficient conditions for universal local structural consistency). *Let the network graph be drawn according to an Erdős-Rényi random graph model, and let \mathbf{A} be a regular diffusion matrix with parameters ρ and κ . Let \mathcal{S} be the set of observable nodes and consider then an estimator $\hat{\mathbf{A}}_{\mathcal{S}} = \mathbf{A}_{\mathcal{S}} + \mathbf{E}$, where \mathbf{E} is the related error matrix. Assume that, for all $i, j \in \mathcal{S}$, with $i \neq j$:*

$$(C.1) \quad \underline{\mathbf{w}}_N \mathbf{a}_{ij} + \underline{\mathbf{z}}_N \leq \mathbf{e}_{ij} \leq \bar{\mathbf{w}}_N \mathbf{a}_{ij} + \bar{\mathbf{z}}_N,$$

where the quantities $\underline{\mathbf{w}}_N$, $\bar{\mathbf{w}}_N$, $\underline{\mathbf{z}}_N$ and $\bar{\mathbf{z}}_N$ do depend on the network size, N , but they do not depend on (i, j) , and fulfill the following convergences:

$$(C.2) \quad \begin{aligned} \underline{\mathbf{w}}_N &\xrightarrow{\text{P}} w, & \bar{\mathbf{w}}_N &\xrightarrow{\text{P}} w, \\ N p_N \underline{\mathbf{z}}_N &\xrightarrow{\text{P}} z, & N p_N \bar{\mathbf{z}}_N &\xrightarrow{\text{P}} z. \end{aligned}$$

Then, under the uniform concentration regime, the estimator $\hat{\mathbf{A}}_{\mathcal{S}}$ achieves universal local structural consistency, with a scaling sequence $s_N = N p_N$, bias $\eta = z$, and identifiability gap $\Gamma = \kappa(1 + w)$.

PROOF. Using the definition of the upper margin in (6.1) we can write:

$$(C.3) \quad \bar{\delta}_N = \max_{\substack{i,j \in \mathcal{S}: \mathbf{a}_{ij}=0 \\ i \neq j}} \hat{\mathbf{a}}_{ij} = \max_{\substack{i,j \in \mathcal{S}: \mathbf{a}_{ij}=0 \\ i \neq j}} \mathbf{e}_{ij},$$

and, hence, from (C.1) we get:

$$(C.4) \quad Np_N \underline{z}_N \leq Np_N \bar{\delta}_N \leq Np_N \bar{z}_N.$$

Using (C.2), we conclude that:

$$(C.5) \quad Np_N \bar{\delta}_N \xrightarrow{P} z.$$

Likewise, recalling the definition of the lower margin in (6.2) we can write:

$$(C.6) \quad \underline{\Delta}_N = \min_{\substack{i,j \in \mathcal{S}: \mathbf{a}_{ij} > 0 \\ i \neq j}} \hat{\mathbf{a}}_{ij} = \min_{\substack{i,j \in \mathcal{S}: \mathbf{a}_{ij} > 0 \\ i \neq j}} (\mathbf{a}_{ij} + \mathbf{e}_{ij}),$$

Now, from (C.1) we know that:

$$(C.7) \quad (1 + \underline{w}_N) \mathbf{a}_{ij} + \underline{z}_N \leq \mathbf{a}_{ij} + \mathbf{e}_{ij} \leq (1 + \bar{w}_N) \mathbf{a}_{ij} + \bar{z}_N,$$

which, used into (C.6), gives:

$$(C.8) \quad Np_N \underline{\Delta}_N \leq (1 + \bar{w}_N) [Np_N \min_{\substack{i,j \in \mathcal{S}: \mathbf{a}_{ij} > 0 \\ i \neq j}} \mathbf{a}_{ij}] + Np_N \bar{z}_N,$$

and

$$(C.9) \quad Np_N \underline{\Delta}_N \geq (1 + \underline{w}_N) [Np_N \min_{\substack{i,j \in \mathcal{S}: \mathbf{a}_{ij} > 0 \\ i \neq j}} \mathbf{a}_{ij}] + Np_N \underline{z}_N.$$

Now we observe that, in view of Assumption 1 we can write, for all pairs (i, j) where $\mathbf{a}_{ij} > 0$:

$$(C.10) \quad \kappa \frac{Np_N}{\mathbf{d}_{\max}} \leq Np_N \mathbf{a}_{ij} \leq \kappa \frac{Np_N}{\mathbf{d}_{\min}},$$

and, hence, under the uniform concentration regime — see (A.10), we conclude from (C.10) that:

$$(C.11) \quad Np_N \min_{\substack{i,j \in \mathcal{S}: \mathbf{a}_{ij} > 0 \\ i \neq j}} \mathbf{a}_{ij} \xrightarrow{P} \kappa,$$

which, used along with (C.2), finally yields:

$$(C.12) \quad Np \underline{\Delta}_N \xrightarrow{P} \kappa(1 + w) + z.$$

It remains to apply the definition of bias and identifiability gap in (6.4) to get the claim of the lemma. \square

In order to prove Theorem 1, it is necessary examine separately the Granger estimator and the other two estimators, namely, the one-lag and the residual estimators.

PROOF FOR THE GRANGER ESTIMATOR. The proof for the Granger estimator boils down to combining Theorem 3 with Lemma 3.

From (7.5) we can write, for $i, j \in \mathcal{S}$, with $i \neq j$:

$$\begin{aligned}
e_{ij}^{(\text{Gra})} &= \sum_{\ell, m \in \mathcal{S}'} \mathbf{a}_{i\ell} \mathbf{h}_{\ell m} \mathbf{a}_{mj}^{(2)} \\
&= \sum_{\ell \in \mathcal{S}'} \mathbf{a}_{i\ell} \mathbf{h}_{\ell\ell} \mathbf{a}_{\ell j}^{(2)} + \sum_{\substack{\ell, m \in \mathcal{S}' \\ \ell \neq m}} \mathbf{a}_{i\ell} \mathbf{h}_{\ell m} \mathbf{a}_{mj}^{(2)} \\
\text{(C.13)} \quad &\leq (1 + \bar{\Sigma}_\alpha) \sum_{\ell \in \mathcal{S}'} \mathbf{a}_{i\ell} \mathbf{a}_{\ell j}^{(2)} \\
&+ \bar{\Sigma}_\beta \sum_{\substack{\ell, m \in \mathcal{S}' \\ \ell \neq m}} \mathbf{a}_{i\ell} \mathbf{a}_{\ell m} \mathbf{a}_{mj}^{(2)} + \bar{\Sigma}_\gamma \sum_{\substack{\ell, m \in \mathcal{S}' \\ \ell \neq m}} \mathbf{a}_{i\ell} \mathbf{a}_{mj}^{(2)}, \\
\text{(C.14)}
\end{aligned}$$

where the inequality is obtained by bounding the entries of the matrix \mathbf{H} , specifically, we have that (C.13) follows from (B.39), whereas (C.14) follows from (B.40). Using now (B.43) in (C.14), we get:

$$\begin{aligned}
e_{ij}^{(\text{Gra})} &\leq (1 + \bar{\Sigma}_\alpha) \sum_{\ell \in \mathcal{S}'} \mathbf{a}_{i\ell} (2 \mathfrak{M}_{a, \text{self}} \mathbf{a}_{\ell j} + \mathfrak{M}) \\
&+ \bar{\Sigma}_\beta \sum_{\substack{\ell, m \in \mathcal{S}' \\ \ell \neq m}} \mathbf{a}_{i\ell} \mathbf{a}_{\ell m} (2 \mathfrak{M}_{a, \text{self}} \mathbf{a}_{mj} + \mathfrak{M}) \\
\text{(C.15)} \quad &+ \bar{\Sigma}_\gamma \sum_{\substack{\ell, m \in \mathcal{S}' \\ \ell \neq m}} \mathbf{a}_{i\ell} (2 \mathfrak{M}_{a, \text{self}} \mathbf{a}_{mj} + \mathfrak{M}),
\end{aligned}$$

which can be recast in the following convenient form:

$$\begin{aligned}
e_{ij}^{(\text{Gra})} &\leq (1 + \bar{\Sigma}_\alpha) \left[2 \mathfrak{M}_{a, \text{self}} \mathfrak{M}^{(S')} + \mathfrak{M} \widetilde{\mathfrak{M}}_{a, \text{sum}}^{(S')} \right] \\
&+ \bar{\Sigma}_\beta \left[2 \mathfrak{M}_{a, \text{self}} \mathfrak{M}_{a_3, \text{sum}}^{(S')} + \mathfrak{M} \widetilde{\mathfrak{M}}^{(S')} \right] \\
&+ \bar{\Sigma}_\gamma \left[2 \mathfrak{M}_{a, \text{self}} \widetilde{\mathfrak{M}}^{(S')} + \mathfrak{M} \widetilde{\mathfrak{M}}_{a, \text{sum}}^{(S')} \right] \triangleq \bar{\mathbf{z}}_N, \\
\text{(C.16)}
\end{aligned}$$

where we have used definitions 7), 8), 9), 10) and 14) listed in Table 3. The arguments leading to this result can be repeated by replacing upper bounds with lower bounds, and maxima with minima (e.g., \mathfrak{M} replaced by \mathfrak{m} , or $\overline{\Sigma}_\alpha$ replaced by $\underline{\Sigma}_\alpha$), yielding:

$$\begin{aligned}
 e_{ij}^{(\text{Gra})} &\geq (1 + \underline{\Sigma}_\alpha) \left[2 \mathfrak{m}_{a,\text{self}} \mathfrak{m}^{(s')} + \mathfrak{m} \tilde{\mathfrak{m}}_{a,\text{sum}}^{(s')} \right] \\
 &+ \underline{\Sigma}_\beta \left[2 \mathfrak{m}_{a,\text{self}} \mathfrak{m}_{a_3,\text{sum}}^{(s')} + \mathfrak{m} \tilde{\mathfrak{m}}^{(s')} \right] \\
 &+ \underline{\Sigma}_\gamma \left[2 \mathfrak{m}_{a,\text{self}} \tilde{\mathfrak{m}}^{(s')} + \mathfrak{m} \tilde{\mathfrak{m}}_{a,\text{sum}}^{(s')} \right] \triangleq \underline{\mathfrak{z}}_N.
 \end{aligned}
 \tag{C.17}$$

Now, under the uniform concentration regime we can use the pertinent convergences in probability listed in Table 3, in conjunction with the convergences in (B.41), which, after some tedious but straightforward algebra, lead to:

$$\boxed{Np_N \bar{\mathfrak{z}}_N \xrightarrow{P} \eta, \quad Np_N \underline{\mathfrak{z}}_N \xrightarrow{P} \eta}
 \tag{C.18}$$

where η is the bias corresponding to the Granger estimator in Table 1. Accordingly, we can conclude that the error for the Granger estimator fulfills the hypotheses of Lemma 3, with the choice $\bar{\mathfrak{w}}_N = \underline{\mathfrak{w}}_N = 0$, and with the quantities $\bar{\mathfrak{w}}_N$ and $\underline{\mathfrak{w}}_N$ defined in (C.16) and (C.17), respectively. This concludes the proof for the claim of the theorem pertaining to the behavior of the Granger estimator under the uniform concentration regime. \square

PROOF FOR THE ONE-LAG AND FOR THE RESIDUAL ESTIMATORS. The proof of the claim for the one-lag and for the residual estimators boils down to combining Theorem 2 with Lemma 3. It suffices to prove the claim for the case $\sigma^2 = 1$, and then scale the bias and the gap by σ^2 .

Using (7.9), the error corresponding to the one-lag estimator can be written as, for all $i, j \in \mathcal{S}$, with $i \neq j$:

$$e_{ij}^{(1\text{-lag})} = \sum_{h=1}^{\infty} \mathfrak{a}_{ij}^{(2h+1)},
 \tag{C.19}$$

and, hence, using the upper and lower bounds in (B.2), along with the definition of the summations in (B.8), we can write:

$$\underline{\Sigma}_\beta^{(\text{odd})} \mathfrak{a}_{ij} + \underline{\Sigma}_\gamma^{(\text{odd})} \mathfrak{m} \leq e_{ij}^{(1\text{-lag})} \leq \overline{\Sigma}_\beta^{(\text{odd})} \mathfrak{a}_{ij} + \overline{\Sigma}_\gamma^{(\text{odd})} \mathfrak{M}.
 \tag{C.20}$$

Now we see that there are two contributions in the error. The first contributions ($\underline{\Sigma}_\beta^{(\text{odd})}$ for the lower bound, and $\overline{\Sigma}_\beta^{(\text{odd})}$ for the upper bound) multiply the entries of the combination matrix, \mathbf{a}_{ij} . Accordingly, they will play a role for connected agents. The second contributions ($\underline{\Sigma}_\gamma^{(\text{odd})} \mathbf{m}$ for the lower bound, and $\overline{\Sigma}_\gamma^{(\text{odd})} \mathfrak{M}$ for the upper bound) play a role for *all* agents, whether or not they are connected.

Now, using the convergence results in (B.12) and in (D.26), simple algebraic calculations lead to:

$$(C.21) \quad Np_N \underline{\Sigma}_\gamma^{(\text{odd})} \mathbf{m} \xrightarrow{P} \eta, \quad Np_N \overline{\Sigma}_\gamma^{(\text{odd})} \mathfrak{M} \xrightarrow{P} \eta,$$

where η is equal to the bias of the one-lag estimator as defined in the pertinent row of Table 1. Likewise, we can prove that:

$$(C.22) \quad \underline{\Sigma}_\beta^{(\text{odd})} \xrightarrow{P} (\psi - 1)\kappa, \quad \overline{\Sigma}_\beta^{(\text{odd})} \xrightarrow{P} (\psi - 1)\kappa,$$

where we introduced the factor:

$$(C.23) \quad \psi \triangleq \frac{1 + (\rho - \kappa)^2}{(1 - (\rho - \kappa)^2)^2}.$$

It remains to apply Lemma 3, with the choices:

$$(C.24) \quad \overline{\mathbf{w}}_N = \overline{\Sigma}_\beta^{(\text{odd})}, \quad \underline{\mathbf{w}}_N = \underline{\Sigma}_\beta^{(\text{odd})},$$

$$(C.25) \quad \overline{\mathbf{z}}_N = \overline{\Sigma}_\gamma^{(\text{odd})} \mathfrak{M}, \quad \underline{\mathbf{z}}_N = \underline{\Sigma}_\gamma^{(\text{odd})} \mathbf{m},$$

which concludes the proof for the one-lag estimator under the uniform concentration regime.

Let us switch to the analysis of the residual estimator. Using (7.13), the error corresponding to the residual estimator can be written as, for all $i, j \in \mathcal{S}$, with $i \neq j$:

$$(C.26) \quad e_{ij}^{(\text{res})} = \sum_{h=1}^{\infty} \mathbf{a}_{ij}^{(2h+1)} - \sum_{h=1}^{\infty} \mathbf{a}_{ij}^{(2h)},$$

and, hence, using the upper and lower bounds in (B.2), along with the definition of the summations in (B.8), we can write:

$$(C.27) \quad e_{ij}^{(\text{res})} \leq (\overline{\Sigma}_\beta^{(\text{odd})} - \underline{\Sigma}_\beta^{(\text{even})}) \mathbf{a}_{ij} + (\overline{\Sigma}_\gamma^{(\text{odd})} \mathfrak{M} - \underline{\Sigma}_\gamma^{(\text{even})} \mathbf{m}),$$

and

$$(C.28) \quad e_{ij}^{(\text{res})} \geq (\underline{\Sigma}_\beta^{(\text{odd})} - \overline{\Sigma}_\beta^{(\text{even})}) \mathbf{a}_{ij} + (\underline{\Sigma}_\gamma^{(\text{odd})} \mathbf{m} - \overline{\Sigma}_\gamma^{(\text{even})} \mathfrak{M}).$$

Now, using the convergence results in (B.12) and in (D.26), simple algebraic calculations lead to:

$$(C.29) \quad \begin{aligned} Np_N (\overline{\Sigma}_\gamma^{(\text{odd})} \mathfrak{M} - \underline{\Sigma}_\gamma^{(\text{even})} \mathfrak{m}) &\xrightarrow{\text{P}} \eta, \\ Np_N (\underline{\Sigma}_\gamma^{(\text{odd})} \mathfrak{m} - \overline{\Sigma}_\gamma^{(\text{even})} \mathfrak{M}) &\xrightarrow{\text{P}} \eta, \end{aligned}$$

where η corresponds to the bias for the residual estimator listed in the pertinent row of Table (1). Likewise, we can prove that:

$$(C.30) \quad \begin{aligned} (\overline{\Sigma}_\beta^{(\text{odd})} - \underline{\Sigma}_\beta^{(\text{even})}) &\xrightarrow{\text{P}} (\psi - 1)\kappa, \\ (\underline{\Sigma}_\beta^{(\text{odd})} - \overline{\Sigma}_\beta^{(\text{even})}) &\xrightarrow{\text{P}} (\psi - 1)\kappa, \end{aligned}$$

where we introduced the factor:

$$(C.31) \quad \psi \triangleq \frac{1}{(1 + \rho - \kappa)^2}.$$

It remains to apply Lemma 3, with the choices:

$$(C.32) \quad \begin{aligned} \overline{\mathbf{w}}_N &= \overline{\Sigma}_\beta^{(\text{odd})} - \underline{\Sigma}_\beta^{(\text{even})}, \\ \underline{\mathbf{w}}_N &= \underline{\Sigma}_\beta^{(\text{odd})} - \overline{\Sigma}_\beta^{(\text{even})}, \end{aligned}$$

and

$$(C.33) \quad \begin{aligned} \overline{\mathbf{z}}_N &= \overline{\Sigma}_\gamma^{(\text{odd})} \mathfrak{M} - \underline{\Sigma}_\gamma^{(\text{even})} \mathfrak{m}, \\ \underline{\mathbf{z}}_N &= \underline{\Sigma}_\gamma^{(\text{odd})} \mathfrak{m} - \overline{\Sigma}_\gamma^{(\text{even})} \mathfrak{M}, \end{aligned}$$

which concludes the proof of the theorem. \square

APPENDIX D: USEFUL CONVERGENCE RESULTS

LEMMA 4 (List of Convergences under Uniform Concentration). *If the connection probability fulfills (5.5), the convergences listed in Table 3 hold true.*

PROOF. 1. We have that:

$$(D.1) \quad \boxed{\mathfrak{M}_{a,\text{self}} \xrightarrow{\text{P}} \rho - \kappa, \quad \mathfrak{m}_{a,\text{self}} \xrightarrow{\text{P}} \rho - \kappa}$$

Since $\mathbf{a}_{ii} = \rho - \sum_{\substack{\ell \in \mathcal{N} \\ \ell \neq i}} \mathbf{a}_{i\ell}$, from (5.8) we can write:

$$(D.2) \quad \mathbf{a}_{ii} \leq \rho - \frac{\kappa}{\mathbf{d}_{\max}} \sum_{\substack{\ell \in \mathcal{N} \\ \ell \neq i}} \mathbf{g}_{i\ell} = \rho - \kappa \frac{\mathbf{d}_i - 1}{\mathbf{d}_{\max}} \leq \rho - \kappa \frac{\mathbf{d}_{\min} - 1}{\mathbf{d}_{\max}}.$$

Therefore, recalling that $\mathfrak{M}_{a,\text{self}} \triangleq \max_{i=1,2,\dots,N} \mathbf{a}_{ii}$, we can write:

$$(D.3) \quad \mathfrak{M}_{a,\text{self}} \leq \rho - \kappa \frac{\mathbf{d}_{\min} - 1}{\mathbf{d}_{\max}}.$$

In view of (A.10), we have that the ratio $\frac{\mathbf{d}_{\min}-1}{\mathbf{d}_{\max}}$ converges to 1 in probability. Repeating the same reasoning with lower bounds in place of upper bounds, and with minima in place of maxima, yields the same result, and, hence, Eq. (D.1) follows.

2. We have that:

$$(D.4) \quad \boxed{\mathfrak{M}_{a_2,\text{self}} \xrightarrow{\text{P}} (\rho - \kappa)^2, \quad \mathfrak{m}_{a_2,\text{self}} \xrightarrow{\text{P}} (\rho - \kappa)^2}$$

We can write:

$$(D.5) \quad \begin{aligned} \mathbf{a}_{ii}^{(2)} &= \sum_{\ell \in \mathcal{N}} \mathbf{a}_{i\ell} \mathbf{a}_{\ell i} = \mathbf{a}_{ii}^2 + \sum_{\substack{\ell \in \mathcal{N} \\ \ell \neq i}} \mathbf{a}_{i\ell} \mathbf{a}_{\ell i} \\ &\leq \mathbf{a}_{ii}^2 + \frac{\kappa^2}{\mathbf{d}_{\min}^2} \sum_{\substack{\ell \in \mathcal{N} \\ \ell \neq i}} \mathbf{g}_{i\ell} \\ &\leq \mathbf{a}_{ii}^2 + \kappa^2 \frac{\mathbf{d}_{\max} - 1}{\mathbf{d}_{\min}^2}, \end{aligned}$$

where the intermediate inequality follows by (5.8). Therefore, recalling that $\mathfrak{M}_{a_2,\text{self}} \triangleq \max_{i \in \mathcal{N}} \mathbf{a}_{ii}^{(2)}$, we can write:

$$(D.6) \quad \mathfrak{M}_{a_2,\text{self}} \leq \mathfrak{M}_{a,\text{self}}^2 + \kappa^2 \frac{\mathbf{d}_{\max} - 1}{\mathbf{d}_{\min}^2},$$

where the last term vanishes in probability in view of (A.10). Using now and (D.1), and repeating the same reasoning with lower bounds in place of upper bounds, and with minima in place of maxima, the result in (D.4) follows.

3. We have that:

$$(D.7) \quad \boxed{\mathfrak{M}_{a,\text{sum}} \xrightarrow{\text{P}} \rho, \quad \mathfrak{m}_{a,\text{sum}} \xrightarrow{\text{P}} \rho}$$

The claim in (D.7) follows readily from the first relationship in (5.8), since we can write, for any $i \neq j$:

$$(D.8) \quad \sum_{\substack{\ell \in \mathcal{N} \\ \ell \neq j}} \mathbf{a}_{i\ell} = \rho - \mathbf{a}_{ij}.$$

In view of (5.8), we have that:

$$(D.9) \quad \mathbf{a}_{ij} \leq \frac{\kappa}{\mathbf{d}_{\min}},$$

and, hence, \mathbf{a}_{ij} goes to zero in probability.

4. We have that:

$$(D.10) \quad \boxed{\mathfrak{M}_{a,\text{sum}}^{(S')} \xrightarrow{\text{P}} \kappa(1 - \xi), \quad \mathfrak{m}_{a,\text{sum}}^{(S')} \xrightarrow{\text{P}} \kappa(1 - \xi)}$$

In view of (5.8) we can write:

$$(D.11) \quad \sum_{\substack{h \in S' \\ h \neq \ell, m}} \mathbf{a}_{hm} \leq \frac{\kappa}{\mathbf{d}_{\min}} \sum_{\substack{h \in S' \\ h \neq \ell, m}} \mathbf{g}_{hm}.$$

Now we observe that the random variable:

$$(D.12) \quad \sum_{\substack{h \in S' \\ h \neq \ell, m}} \mathbf{g}_{hm}$$

is a binomial random variable with number of trials equal to $S' - 2$, and success probability equal to p_N . In other words, we get the following representation:

$$(D.13) \quad \max_{\substack{\ell, m \in S' \\ \ell \neq m}} \sum_{\substack{h \in S' \\ h \neq \ell, m}} \mathbf{g}_{hm} = \mathcal{B}_{\max}(S' - 2, p_N, (S' - 1)S'),$$

because maximization is carried over all pairs $\ell, m \in S'$, with $\ell \neq m$. Moreover, since in the uniform concentration regime we have

$$(D.14) \quad p_N = \omega_N \frac{\log N}{N}, \quad \omega_N \xrightarrow{N \rightarrow \infty} \infty,$$

and since $S'/N \rightarrow 1 - \xi$ as $N \rightarrow \infty$, we can regard the connection probability p_N as a connection probability scaling with respect to S' , namely,

$$\begin{aligned} p_N &= \omega_N \frac{\log(S')}{S'} \frac{S'}{N} \frac{\log N}{\log(S'/N) + \log N} \\ (D.15) \quad &= \omega_{S'} \frac{\log(S')}{S'} \triangleq p_{S'}, \end{aligned}$$

where

$$(D.16) \quad \omega_{S'} = \omega_N \frac{S'}{N} \frac{\log N}{\log(S'/N) + \log N} \xrightarrow{N \rightarrow \infty} \infty.$$

This shows that the uniform concentration regime can be referred also to the scaling of the involved quantities w.r.t. S' (in place of N). Accordingly, we can apply (A.3) with $K = (S' - 1)S'$, $N = S' - 2$, and $p_{S'} = \omega_{S'} \log(S')/S'$, which yields:

$$(D.17) \quad \frac{\mathcal{B}_{\max}(S' - 2, p_N, (S' - 1)S')}{S'p_N} \xrightarrow{p} 1.$$

It remains to rewrite (D.11) as:

$$\begin{aligned} \sum_{\substack{h \in S' \\ h \neq \ell, m}} \mathbf{a}_{hm} &\leq \kappa \underbrace{\frac{Np_N}{\mathbf{d}_{\min}}}_{\xrightarrow{p} 1} \underbrace{\frac{S'}{N}}_{\rightarrow 1 - \xi} \\ &\times \underbrace{\frac{\mathcal{B}_{\max}(S' - 2, p_N, (S' - 1)S')}{S'p_N}}_{\xrightarrow{p} 1}. \end{aligned} \quad (D.18)$$

Repeating the same reasoning with lower bounds in place of upper bounds, and with minima in place of maxima, yields the same result, and, hence, Eqs. (D.10) follow.

5. We have that:

$$(D.19) \quad \boxed{\mathfrak{M}_{c,\text{self}} \xrightarrow{p} (\rho - \kappa)^2, \quad \mathfrak{m}_{c,\text{self}} \xrightarrow{p} (\rho - \kappa)^2}$$

This result follows readily by repeating the same steps used to prove (D.4).

6. We have that:

$$(D.20) \quad \boxed{\begin{aligned} \mathfrak{M}_{c,\text{sum}} &\xrightarrow{p} \rho^2 - 2\rho\kappa\xi + \kappa^2\xi, \\ \mathfrak{m}_{c,\text{sum}} &\xrightarrow{p} \rho^2 - 2\rho\kappa\xi + \kappa^2\xi \end{aligned}}$$

Using the definition of \mathbf{C} in (7.4), we note that we can write:

$$\begin{aligned}
 \sum_{\substack{h \in \mathcal{S}' \\ h \neq m}} \mathbf{c}_{lh} &= \sum_{\substack{h \in \mathcal{S}' \\ h \neq m}} \sum_{j \in \mathcal{N}} \mathbf{a}_{lj} \mathbf{a}_{jh} \\
 &= \sum_{j \in \mathcal{S}} \mathbf{a}_{lj} \sum_{\substack{h \in \mathcal{S}' \\ h \neq m}} \mathbf{a}_{jh} + \sum_{j \in \mathcal{S}'} \mathbf{a}_{lj} \sum_{\substack{h \in \mathcal{S}' \\ h \neq m}} \mathbf{a}_{jh}.
 \end{aligned}
 \tag{D.21}$$

Applying the same procedure used in the previous items of this section, it is readily proved that, if $j \in \mathcal{S}$ (and, hence the self-term $\mathbf{a}_{\ell\ell}$ is not present, because $\ell \in \mathcal{S}'$):

$$\max_{j \in \mathcal{S}} \sum_{\substack{h \in \mathcal{S}' \\ h \neq m}} \mathbf{a}_{jh} \xrightarrow{\text{P}} \kappa(1 - \xi), \quad \min_{j \in \mathcal{S}} \sum_{\substack{h \in \mathcal{S}' \\ h \neq m}} \mathbf{a}_{jh} \xrightarrow{\text{P}} \kappa(1 - \xi),
 \tag{D.22}$$

whereas, if $j \in \mathcal{S}'$:

$$\max_{j \in \mathcal{S}} \sum_{\substack{h \in \mathcal{S}' \\ h \neq m}} \mathbf{a}_{jh} \xrightarrow{\text{P}} \rho - \kappa\xi, \quad \min_{j \in \mathcal{S}} \sum_{\substack{h \in \mathcal{S}' \\ h \neq m}} \mathbf{a}_{jh} \xrightarrow{\text{P}} \rho - \kappa\xi.
 \tag{D.23}$$

Likewise, we can show that:

$$\max_{\ell \in \mathcal{S}'} \sum_{j \in \mathcal{S}} \mathbf{a}_{\ell j} \xrightarrow{\text{P}} \kappa\xi, \quad \min_{\ell \in \mathcal{S}'} \sum_{j \in \mathcal{S}} \mathbf{a}_{\ell j} \xrightarrow{\text{P}} \kappa\xi,
 \tag{D.24}$$

and that:

$$\max_{\ell \in \mathcal{S}'} \sum_{j \in \mathcal{S}'} \mathbf{a}_{\ell j} \xrightarrow{\text{P}} \rho - \kappa\xi, \quad \min_{\ell \in \mathcal{S}'} \sum_{j \in \mathcal{S}'} \mathbf{a}_{\ell j} \xrightarrow{\text{P}} \rho - \kappa\xi.
 \tag{D.25}$$

Plugging (D.22)–(D.25) into (D.21) finally yields (D.20).

7. We have that:

$$\boxed{Np_N \mathfrak{M} \xrightarrow{\text{P}} \kappa^2 p, \quad Np_N \mathfrak{m} \xrightarrow{\text{P}} \kappa^2 p}
 \tag{D.26}$$

In view of (5.8), we can write:

$$\sum_{\substack{\ell \in \mathcal{N} \\ \ell \neq i, j}} \mathbf{a}_{i\ell} \mathbf{a}_{\ell j} \leq \frac{\kappa^2}{d_{\min}^2} \sum_{\substack{\ell \in \mathcal{N} \\ \ell \neq i, j}} \mathbf{g}_{i\ell} \mathbf{g}_{\ell j}.
 \tag{D.27}$$

Now we see that the quantity:

$$(D.28) \quad \sum_{\substack{\ell \in \mathcal{N} \\ \ell \neq i,j}} \mathbf{g}_{i\ell} \mathbf{g}_{\ell j}$$

is a binomial random variable with number of trials equal to $N - 2$, and success probability equal to p_N^2 , since when $\ell \neq i, j$, the product variable $\mathbf{g}_{i\ell} \mathbf{g}_{\ell j}$ is a Bernoulli variable with success probability p_N^2 . Therefore, we are allowed to introduce the definition:

$$(D.29) \quad \mathcal{B}_{\max}(N - 2, p_N^2, (N - 1)N) = \max_{\substack{i,j \in \mathcal{N} \\ i \neq j}} \sum_{\substack{\ell \in \mathcal{N} \\ \ell \neq i,j}} \mathbf{g}_{i\ell} \mathbf{g}_{\ell j},$$

which, in view of Lemma 2, yields:

$$(D.30) \quad \frac{1}{Np_N} \max_{\substack{i,j \in \mathcal{N} \\ i \neq j}} \sum_{\ell \neq i,j} \mathbf{g}_{i\ell} \mathbf{g}_{\ell j} \xrightarrow{p} p.$$

Now, from the definition of \mathfrak{M} in Table 3, line 12), we get:

$$(D.31) \quad Np_N \mathfrak{M} \leq \kappa^2 \underbrace{\frac{\mathcal{B}_{\max}(N - 2, p_N^2, (N - 1)N)}{Np_N}}_{\xrightarrow{p} p} \underbrace{\frac{N^2 p_N^2}{\mathbf{d}_{\min}^2}}_{\xrightarrow{p} 1}.$$

Repeating the same reasoning with lower bounds in place of upper bounds, and with minima in place of maxima, we get the claim in (D.26).

8. We have that:

$$(D.32) \quad \boxed{\begin{array}{l} Np_N \mathfrak{M}^{(S')} \xrightarrow{p} \kappa^2 p(1 - \xi), \\ Np_N \mathfrak{m}^{(S')} \xrightarrow{p} \kappa^2 p(1 - \xi) \end{array}}$$

The proof for the case where $p = 0$ comes from (D.26) because, from definitions 12) and 13) in Table 3, we see that $\mathfrak{M}^{(S')} \leq \mathfrak{M}$. The proof for the case where $p > 0$ is readily obtained by using the same arguments leading to (D.26).

9. We have that:

$$(D.33) \quad \boxed{\begin{array}{l} Np_N \mathfrak{M}_{a_3, \text{sum}}^{(S')} \xrightarrow{p} \kappa^3 p(1 - \xi)^2, \\ Np_N \mathfrak{m}_{a_3, \text{sum}}^{(S')} \xrightarrow{p} \kappa^3 p(1 - \xi)^2 \end{array}}$$

We have that:

$$\begin{aligned}
 & \sum_{\substack{\ell, m \in \mathcal{S}' \\ \ell \neq m}} \mathbf{a}_{i\ell} \mathbf{a}_{\ell m} \mathbf{a}_{mj} \\
 &= \sum_{\ell \in \mathcal{S}'} \mathbf{a}_{i\ell} \sum_{\substack{m \in \mathcal{S}' \\ m \neq \ell}} \mathbf{a}_{\ell m} \mathbf{a}_{mj} \\
 \text{(D.34)} \quad &\leq \max_{i \in \mathcal{S}} \sum_{\ell \in \mathcal{S}'} \mathbf{a}_{i\ell} \max_{j \in \mathcal{S}, \ell \in \mathcal{S}'} \sum_{\substack{m \in \mathcal{S}' \\ m \neq \ell}} \mathbf{a}_{\ell m} \mathbf{a}_{mj}.
 \end{aligned}$$

Reasoning as done for proving (D.32), we can show that:

$$\text{(D.35)} \quad N p_N \max_{j \in \mathcal{S}, \ell \in \mathcal{S}'} \sum_{\substack{m \in \mathcal{S}' \\ m \neq \ell}} \mathbf{a}_{\ell m} \mathbf{a}_{mj} \xrightarrow{\text{P}} \kappa^2 p(1 - \xi).$$

Likewise, reasoning as done for proving (D.10), we can show that:

$$\text{(D.36)} \quad \max_{i \in \mathcal{S}} \sum_{\ell \in \mathcal{S}'} \mathbf{a}_{i\ell} \xrightarrow{\text{P}} \kappa(1 - \xi).$$

Finally, using (D.35) and (D.36) into (D.34), repeating the same reasoning with lower bounds in place of upper bounds, and with minima in place of maxima, we get (D.33).

10. The following list of convergences is obtained by trivial variations on the previous proofs.

$$\text{(D.37)} \quad \boxed{\widetilde{\mathfrak{M}}^{(\mathcal{S}')} \xrightarrow{\text{P}} \kappa^2(1 - \xi)^2, \quad \widetilde{\mathfrak{m}}^{(\mathcal{S}')} \xrightarrow{\text{P}} \kappa^2(1 - \xi)^2}$$

$$\text{(D.38)} \quad \boxed{\widetilde{\mathfrak{M}}^{(\mathcal{S}')} \xrightarrow{\text{P}} \kappa^2(1 - \xi)^2, \quad \widetilde{\mathfrak{m}}^{(\mathcal{S}')} \xrightarrow{\text{P}} \kappa^2(1 - \xi)^2}$$

$$\text{(D.39)} \quad \boxed{\widetilde{\mathfrak{M}}_{a, \text{sum}}^{(\mathcal{S}')} \xrightarrow{\text{P}} \kappa(1 - \xi), \quad \widetilde{\mathfrak{m}}_{a, \text{sum}}^{(\mathcal{S}')} \xrightarrow{\text{P}} \kappa(1 - \xi)}$$

$$\text{(D.40)} \quad \boxed{\widetilde{\mathfrak{M}}_{a, \text{sum}}^{(\mathcal{S}')} \xrightarrow{\text{P}} \kappa(1 - \xi)^2, \quad \widetilde{\mathfrak{m}}_{a, \text{sum}}^{(\mathcal{S}')} \xrightarrow{\text{P}} \kappa(1 - \xi)^2}$$

□

APPENDIX E: USEFUL LEMMA

LEMMA 5. *Let $0 < \alpha < 1$, $0 < \rho_\ell < 1$ and $\beta_\ell \in \mathbb{R}$ for all $\ell = 1, 2, \dots, L$, and introduce the following recursion:*

$$(E.1) \quad f_{k+1} = \alpha f_k + \sum_{\ell=1}^L \beta_\ell \rho_\ell^k.$$

Then, f_k is equal to:

$$(E.2) \quad \left(f_0 + \sum_{\ell=1}^L \frac{\beta_\ell}{\alpha - \rho_\ell} \right) \alpha^k - \sum_{\ell=1}^L \frac{\beta_\ell}{\alpha - \rho_\ell} \rho_\ell^k,$$

and, hence, can be cast in the following form:

$$(E.3) \quad f_k = \sum_{\ell=0}^L \tilde{\beta}_\ell \tilde{\rho}_\ell^k,$$

with obvious choices for $\tilde{\beta}_\ell$ and $\tilde{\rho}_\ell$.

PROOF. Exploiting (E.2), we can write:

$$(E.4) \quad \begin{aligned} f_1 &= \alpha f_0 + \sum_{\ell=1}^L \beta_\ell, \\ f_2 &= \alpha^2 f_0 + \alpha \sum_{\ell=1}^L \beta_\ell + \sum_{\ell=1}^L \beta_\ell \rho_\ell, \\ &\vdots \\ f_k &= \alpha^k f_0 + \sum_{\ell=1}^L \beta_\ell \sum_{j=0}^{k-1} \alpha^{k-1-j} \rho_\ell^j. \end{aligned}$$

The last equation can be manipulated as follows:

$$(E.5) \quad \begin{aligned} f_k &= \alpha^k f_0 + \sum_{\ell=1}^L \beta_\ell \alpha^{k-1} \sum_{j=0}^{k-1} \left(\frac{\rho_\ell}{\alpha} \right)^j \\ &= \alpha^k f_0 + \sum_{\ell=1}^L \beta_\ell \alpha^{k-1} \frac{1 - (\rho_\ell/\alpha)^k}{1 - \rho_\ell/\alpha} \\ &= \alpha^k f_0 + \sum_{\ell=1}^L \beta_\ell \frac{\alpha^k - \rho_\ell^k}{\alpha - \rho_\ell}, \end{aligned}$$

which corresponds to (E.2). \square

REFERENCES

- [1] ANANDKUMAR, A., TAN, V. Y. F., HUANG, F. and WILLSKY, A. S. (2012). High-dimensional Gaussian graphical model selection: Walk summability and local separation criterion. *Journal of Machine Learning Research* **13** 2293-2337.
- [2] ANANDKUMAR, A. and VALLUVAN, R. (2013). Learning loopy graphical models with latent variables: Efficient methods and guarantees. *The Annals of Statistics* **41** 401-435.
- [3] BAJOVIC, D., JAKOVETIC, D., XAVIER, J., SINOPOLI, B. and MOURA, J. M. F. (2011). Distributed detection via Gaussian running consensus: Large deviations asymptotic analysis. *IEEE Transactions on Signal Processing* **59** 4381-4396.
- [4] BARRAT, A., BARTHÉLEMY, M. and VESPIGNANI, A. (2012). *Dynamical Processes on Complex Networks*. Cambridge University Press.
- [5] BENTO, J. and MONTANARI, A. (2009). Which graphical models are difficult to learn? In *Proc. International Conference on Neural Information Processing Systems (NIPS)* 1303-1311.
- [6] BOLLOBÁS, B. (2001). *Random Graphs*. Cambridge University Press.
- [7] BOUCHERON, S., LUGOSI, G. and MASSART, P. (2013). *Concentration Inequalities: A Nonasymptotic Theory of Independence*. Oxford University Press.
- [8] BOYD, S., GHOSH, A., PRABHAKAR, B. and SHAH, D. (2006). Randomized gossip algorithms. *IEEE Transactions on Information Theory* **52** 2508-2530.
- [9] BRESLER, G., GAMARNIK, D. and SHAH, D. (2014). Hardness of parameter estimation in graphical models. In *Proc. Neural Information Processing Systems (NIPS)* 1062-1070. MIT Press.
- [10] CHANDRASEKARAN, V., PARRILO, P. A. and WILLSKY, A. S. (2012). Latent variable graphical model selection via convex optimization. *The Annals of Statistics* **40** 1935-1967.
- [11] CHERAGHCHI, M., KARBASI, A., MOHAJER, S. and SALIGRAMA, V. (2012). Graph-constrained group testing. *IEEE Transactions on Information Theory* **58** 248-262.
- [12] CHICKERING, D. M., HECKERMAN, D. and MEEK, C. (2004). Large-sample learning of Bayesian networks is NP-hard. *Journal of Machine Learning Research* **5** 1287-1330.
- [13] DIMAKIS, A. G., KAR, S., MOURA, J. M. F., RABBAT, M. G. and SCAGLIONE, A. (2010). Gossip algorithms for distributed signal processing. *Proceedings of the IEEE* **98** 1847-1864.
- [14] ERDŐS, P. and RÉNYI, A. (1959). On random graphs I. *Publicationes Mathematicae (Debrecen)* **6** 290-297.
- [15] ETESAMI, J. and KIYAVASH, N. (2017). Measuring causal relationships in dynamical systems through recovery of functional dependencies. *IEEE Transactions on Signal and Information Processing over Networks* **3** 650-659.
- [16] ETESAMI, J., KIYAVASH, N. and COLEMAN, T. (2016). Learning minimal latent directed information polytrees. *Neural Computation* **28** 1723-1768.
- [17] GEIGER, P., ZHANG, K., SCHÖLKOPF, B., GONG, M. and JANZING, D. (2015). Causal inference by identification of vector autoregressive processes with hidden components. In *Proc. International Conference on Machine Learning* **37** 1917-1925.
- [18] HONEY, C. J., SPORNS, O., CAMMOUN, L., GIGANDET, X., THIRAN, J. P., MEULI, R. and HAGMANN, P. (2009). Predicting human resting-state functional connectivity

- from structural connectivity. *Proceedings of the National Academy of Sciences* **106** 2035–2040.
- [19] MAHDIZADEHAGHDAM, S., WANG, H., KRIM, H. and DAI, L. (2016). Information diffusion of topic propagation in social media. *IEEE Transactions on Signal and Information Processing over Networks* **2** 569–581.
- [20] MATEOS, G., SEGARRA, S., MARQUES, A. and RIBEIRO, A. (2018). Connecting the dots: Identifying network structure via graph signal processing. *submitted for publication*, available online as [arXiv:1810.13066v1](https://arxiv.org/abs/1810.13066v1) [eess.SP].
- [21] MATERASSI, D. and SALAPAKA, M. V. (2012). On the problem of reconstructing an unknown topology via locality properties of the Wiener filter. *IEEE Transactions on Automatic Control* **57** 1765–1777.
- [22] MATERASSI, D. and SALAPAKA, M. V. (2012). Network reconstruction of dynamical polytrees with unobserved nodes. In *Proc. IEEE Conference on Decision and Control (CDC)* 4629–4634.
- [23] MATERASSI, D. and SALAPAKA, M. V. (2015). Identification of network components in presence of unobserved nodes. In *Proc. IEEE Conference on Decision and Control (CDC)* 1563–1568.
- [24] MATTA, V., SANTOS, A. and SAYED, A. H. (2018). Tomography of large adaptive networks under the dense latent regime. In *Proc. IEEE Asilomar Conference on Signals, Systems and Computers* 2144–2148.
- [25] MATTA, V., SANTOS, A. and SAYED, A. H. (2019). Graph learning with partial observations: Role of degree concentration. In *Proc. IEEE International Symposium on Information Theory (ISIT)* 1–5.
- [26] MATTA, V. and SAYED, A. H. (2018). Tomography of adaptive multi-agent networks under limited observation. In *Proc. IEEE International Conference on Acoustics, Speech and Signal Processing (ICASSP)* 6638–6642.
- [27] MATTA, V. and SAYED, A. H. (2018). Estimation and detection over adaptive networks. In *Cooperative and Graph Signal Processing* (P. Djuric and C. Richard, eds.) 69–106. Elsevier.
- [28] MATTA, V. and SAYED, A. H. (2019). Consistent tomography under partial observations over adaptive networks. *IEEE Transactions on Information Theory* **65** 622–646.
- [29] MAUROY, A. and GONCALVES, J. (2016). Linear identification of nonlinear systems: A lifting technique based on the Koopman operator. In *Proc. IEEE Conference on Decision and Control (CDC)* 6500–6505.
- [30] MEI, J. and MOURA, J. (2017). Signal processing on graphs: Causal modeling of unstructured data. *IEEE Transactions on Signal Processing* **65** 2077–2092.
- [31] MONETA, A., CHLASS, N., ENTNER, D. and HOYER, P. (2009). Causal search in structural vector autoregressive models. In *Proc. International Conference on Neural Information Processing Systems (NIPS)* 95–118.
- [32] NAPOLETANI, D. and SAUER, T. D. (2008). Reconstructing the topology of sparsely connected dynamical networks. *Physical Review E* **77** 026103.
- [33] PASDELOUP, B., GRIPON, V., MERCIER, G., PASTOR, D. and RABBAT, M. G. (2018). Characterization and inference of graph diffusion processes from observations of stationary signals. *IEEE Transactions on Signal and Information Processing over Networks* **4** 481–496.
- [34] PINTO, P. C., THIRAN, P. and VETTERLI, M. (2012). Locating the source of diffusion in large-scale networks. *Physical Review Letters* **109** 068702.

- [35] QUINN, C. J., KIYAVASH, N. and COLEMAN, T. P. (2015). Directed information graphs. *IEEE Transactions on Information Theory* **61** 6887-6909.
- [36] SANTOS, A., MATTA, V. and SAYED, A. H. (2018). Local tomography of large networks under the low-observability regime. *submitted for publication*, available online as [arXiv:1805.09081](https://arxiv.org/abs/1805.09081)v1 [cs.MA].
- [37] SANTOS, A., MATTA, V. and SAYED, A. H. (2018). Divide-and-conquer tomography for large-scale networks. In *Proc. IEEE Data Science Workshop* 170-174.
- [38] SANTOS, A., MATTA, V. and SAYED, A. H. (2018). Consistent tomography over diffusion networks under the low-observability regime. In *Proc. IEEE International Symposium on Information Theory* 1839-1843.
- [39] SAYED, A. H. (2014). Adaptive networks. *Proceedings of the IEEE* **102** 460-497.
- [40] SEGARRA, S., SCHAUB, M. T. and JADBABAIE, A. (2017). Network inference from consensus dynamics. In *Proc. IEEE Conference on Decision and Control (CDC)* 3212-3217.
- [41] VENKITASUBRAMANIAM, P., HE, T. and TONG, L. (2008). Anonymous networking amidst eavesdroppers. *IEEE Transactions on Information Theory* **54** 2770-2784.

DIEM, UNIVERSITY OF SALERNO,
VIA GIOVANNI PAOLO II, I-84084,
FISCIANO (SA), ITALY
E-MAIL: vmatta@unisa.it

ÉCOLE POLYTECHNIQUE FÉDÉRALE DE LAUSANNE,
SCHOOL OF ENGINEERING,
CH-1015 LAUSANNE, SWITZERLAND
E-MAIL: augusto.santos@epfl.ch
ali.sayed@epfl.ch

	Random variable	Random variable	Limit (in probability)
1)	$\mathfrak{M}_a \triangleq \max_{\substack{i,j \in \mathcal{N} \\ i \neq j}} \mathbf{a}_{ij}$	$\mathfrak{m}_a \triangleq \min_{\substack{i,j \in \mathcal{N} \\ i \neq j}} \mathbf{a}_{ij}$	0
2)	$\mathfrak{M}_{a,\text{self}} \triangleq \max_{i \in \mathcal{N}} \mathbf{a}_{ii}$	$\mathfrak{m}_{a,\text{self}} \triangleq \min_{i \in \mathcal{N}} \mathbf{a}_{ii}$	$\rho - \kappa$
3)	$\mathfrak{M}_{a_2,\text{self}} \triangleq \max_{i \in \mathcal{N}} \mathbf{a}_{ii}^{(2)}$	$\mathfrak{m}_{a_2,\text{self}} \triangleq \min_{i \in \mathcal{N}} \mathbf{a}_{ii}^{(2)}$	$(\rho - \kappa)^2$
4)	$\mathfrak{M}_{a,\text{sum}} \triangleq \max_{\substack{i,j \in \mathcal{N} \\ i \neq j}} \sum_{\substack{\ell \in \mathcal{N} \\ \ell \neq j}} \mathbf{a}_{i\ell}$	$\mathfrak{m}_{a,\text{sum}} \triangleq \min_{\substack{i,j \in \mathcal{N} \\ i \neq j}} \sum_{\substack{\ell \in \mathcal{N} \\ \ell \neq j}} \mathbf{a}_{i\ell}$	ρ
5)	$\mathfrak{M}_{c,\text{self}} \triangleq \max_{\ell \in \mathcal{S}'} \mathbf{c}_{\ell\ell}$	$\mathfrak{m}_{c,\text{self}} \triangleq \min_{\ell \in \mathcal{S}'} \mathbf{c}_{\ell\ell}$	$(\rho - \kappa)^2$
6)	$\mathfrak{M}_{a,\text{sum}}^{(s')} \triangleq \max_{\substack{\ell, m \in \mathcal{S}' \\ \ell \neq m}} \sum_{\substack{h \in \mathcal{S}' \\ h \neq \ell, m}} \mathbf{a}_{hm}$	$\mathfrak{m}_{a,\text{sum}}^{(s')} \triangleq \min_{\substack{\ell, m \in \mathcal{S}' \\ \ell \neq m}} \sum_{\substack{h \in \mathcal{S}' \\ h \neq \ell, m}} \mathbf{a}_{hm}$	$\kappa(1 - \xi)$
7)	$\widetilde{\mathfrak{M}}_{a,\text{sum}}^{(s')} \triangleq \max_{i \in \mathcal{S}} \sum_{\ell \in \mathcal{S}'} \mathbf{a}_{i\ell}$	$\widetilde{\mathfrak{m}}_{a,\text{sum}}^{(s')} \triangleq \min_{i \in \mathcal{S}} \sum_{\ell \in \mathcal{S}'} \mathbf{a}_{i\ell}$	$\kappa(1 - \xi)$
8)	$\widetilde{\widetilde{\mathfrak{M}}}_{a,\text{sum}}^{(s')} \triangleq \max_{i \in \mathcal{S}} \sum_{\substack{\ell, m \in \mathcal{S}' \\ \ell \neq m}} \mathbf{a}_{i\ell}$	$\widetilde{\widetilde{\mathfrak{m}}}_{a,\text{sum}}^{(s')} \triangleq \min_{i \in \mathcal{S}} \sum_{\substack{\ell, m \in \mathcal{S}' \\ \ell \neq m}} \mathbf{a}_{i\ell}$	$\kappa(1 - \xi)^2$
9)	$\widetilde{\widetilde{\mathfrak{M}}}^{(s')} \triangleq \max_{i \in \mathcal{S}} \sum_{\substack{\ell, m \in \mathcal{S}' \\ \ell \neq m}} \mathbf{a}_{i\ell} \mathbf{a}_{\ell m}$	$\widetilde{\widetilde{\mathfrak{m}}}^{(s')} \triangleq \min_{i \in \mathcal{S}} \sum_{\substack{\ell, m \in \mathcal{S}' \\ \ell \neq m}} \mathbf{a}_{i\ell} \mathbf{a}_{\ell m}$	$\kappa^2(1 - \xi)^2$
10)	$\widetilde{\mathfrak{M}}^{(s')} \triangleq \max_{\substack{i,j \in \mathcal{S} \\ i \neq j}} \sum_{\substack{\ell, m \in \mathcal{S}' \\ \ell \neq m}} \mathbf{a}_{i\ell} \mathbf{a}_{mj}$	$\widetilde{\mathfrak{m}}^{(s')} \triangleq \min_{\substack{i,j \in \mathcal{S} \\ i \neq j}} \sum_{\substack{\ell, m \in \mathcal{S}' \\ \ell \neq m}} \mathbf{a}_{i\ell} \mathbf{a}_{mj}$	$\kappa^2(1 - \xi)^2$
11)	$\mathfrak{M}_{c,\text{sum}} \triangleq \max_{\substack{\ell, m \in \mathcal{S}' \\ \ell \neq m}} \sum_{\substack{h \in \mathcal{S}' \\ h \neq m}} \mathbf{c}_{\ell h}$	$\mathfrak{m}_{c,\text{sum}} \triangleq \min_{\substack{\ell, m \in \mathcal{S}' \\ \ell \neq m}} \sum_{\substack{h \in \mathcal{S}' \\ h \neq m}} \mathbf{c}_{\ell h}$	$\rho^2 - 2\rho\kappa\xi + \kappa^2\xi$
12)	$\mathfrak{M} \triangleq \max_{\substack{i,j \in \mathcal{N} \\ i \neq j}} \sum_{\substack{\ell \in \mathcal{N} \\ \ell \neq i,j}} \mathbf{a}_{i\ell} \mathbf{a}_{\ell j}$	$\mathfrak{m} \triangleq \min_{\substack{i,j \in \mathcal{N} \\ i \neq j}} \sum_{\substack{\ell \in \mathcal{N} \\ \ell \neq i,j}} \mathbf{a}_{i\ell} \mathbf{a}_{\ell j}$	$\left. \begin{array}{l} Np_N \mathfrak{M} \\ Np_N \mathfrak{m} \end{array} \right\} \xrightarrow{p} \kappa^2 p$
13)	$\mathfrak{M}^{(s')} \triangleq \max_{\substack{i,j \in \mathcal{N} \\ i \neq j}} \sum_{\substack{\ell \in \mathcal{S}' \\ \ell \neq i,j}} \mathbf{a}_{i\ell} \mathbf{a}_{\ell j}$	$\mathfrak{m}^{(s')} \triangleq \min_{\substack{i,j \in \mathcal{N} \\ i \neq j}} \sum_{\substack{\ell \in \mathcal{S}' \\ \ell \neq i,j}} \mathbf{a}_{i\ell} \mathbf{a}_{\ell j}$	$\left. \begin{array}{l} Np_N \mathfrak{M}^{(s')} \\ Np_N \mathfrak{m}^{(s')} \end{array} \right\} \xrightarrow{p} \kappa^2 p(1 - \xi)$
14)	$\mathfrak{M}_{a_3,\text{sum}}^{(s')} \triangleq \max_{\substack{i,j \in \mathcal{S} \\ i \neq j}} \sum_{\substack{\ell, m \in \mathcal{S}' \\ \ell \neq m}} \mathbf{a}_{i\ell} \mathbf{a}_{\ell m} \mathbf{a}_{mj}$	$\mathfrak{m}_{a_3,\text{sum}}^{(s')} \triangleq \min_{\substack{i,j \in \mathcal{S} \\ i \neq j}} \sum_{\substack{\ell, m \in \mathcal{S}' \\ \ell \neq m}} \mathbf{a}_{i\ell} \mathbf{a}_{\ell m} \mathbf{a}_{mj}$	$\left. \begin{array}{l} Np_N \mathfrak{M}_{a_3,\text{sum}}^{(s')} \\ Np_N \mathfrak{m}_{a_3,\text{sum}}^{(s')} \end{array} \right\} \xrightarrow{p} \kappa^3 p(1 - \xi)^2$

TABLE 3

Random variables and convergences relevant for the proofs of the theorems.